Ionization effects in the inner electron shells of ionized atoms

G. Zschornack

Joint Institute for Nuclear Research, Dubna, and Technical University, Dresden
Fiz. Elem. Chastits At. Yadra **14**, 835–899 (July–August 1983)

The physics of the atomic shells of ionized atoms is reviewed. Interaction effects and structural effects in the atomic shells associated with vacancies in different subshells are considered. Methods of calculating the parameters of the atomic structures and wave functions are described. The dependence of the energy of the characteristic x rays emitted by the ions on the degree of their ionization is analyzed. The influence of vacancies in the outer and inner shells of an atom on the x-ray energy is described in detail. The influence of chemical valence states on the x-ray parameters is discussed. The dependence of the probabilities of radiative and nonradiative electron transitions on the degree of ionization is considered, and the parts played by Auger and Coster–Kronig processes in the rearrangement of the atomic shells are elucidated. The influence of nonradiative electron transitions on the cross sections of multiple ionization is estimated. The ionization cross sections for direct and indirect processes are given for ions of different charge states.

PACS numbers: 32.30.Rj, 34.50.Hc

INTRODUCTION

During the last decades, interest in the processes and interactions in the atomic shells of ionized atoms has increased considerably. The shell physics of ionized atoms has been the subject of numerous theoretical and experimental papers. The reasons for the steadily growing attention paid to this previously little studied field of atomic physics are above all the terrestrial and extraterrestrial objects and phenomena studied in modern physics for which processes in ionized atoms are important. There are facilities that depend functionally on the presence of more or less strongly ionized atoms. The practical realization of the acceleration of heavy ions and the development of heavy-ion physics make the investigation of multiply ionized atoms very important. Effects associated with ionization processes in atomic shells acquire great importance in research facilities and prototypes of controlled thermonuclear fusion reactors. The need for atomic and molecular data, in particular for multiply ionized atoms, has been emphasized at working sessions of the IAEA.[1,2]

Ionized atomic states influence many properties of the plasma that will be used in future thermonuclear fusion reactors. For simulation of the plasma (energy loss, particle transport, density of particles, instabilities) great importance attaches to processes such as excitation of atoms by electrons, ionization of the atoms by electrons, charge-exchange and recombination processes, and electron–ion and ion–ion collisions. For plasma diagnostics (temperature and density of the particles and impurities, influence of the plasma on constructional materials) it is necessary to know the energy and intensities of the lines of the characteristic x-ray emission of the ionized atoms and the ionization potentials for the electrons of all subshells and arbitrary degrees of ionization of the atoms. Reliable diagnostics of thermonuclear plasmas is particularly important, since even a fraction of a percent of impurities significantly influences the energy loss, transport processes, and stability of plasmas.[3]

With the expansion of hot-plasma research under laboratory conditions, atomic physicists take an increasing interest in the study of plasmas in the optical range and in the region of the characteristic and continuum x-ray emission. These components of the emission are important from the point of view of the energy losses, but they also give valuable possibilities for plasma diagnostics.

In the last decades, spectrometry of x-ray radiation of extraterrestrial origin has been developed. Discrete x-ray sources and a diffuse radiation background have been discovered. The x-ray energy spectrum of extraterrestrial sources is similar to the spectrum of terrestrial laboratory plasma sources, and in a number of cases it is produced by the emission of multiply charged ions.

The x-ray source nearest the Earth is the Sun. The solar protuberances are sources of short-wave x rays and accelerated particles.[4] In the spectrum of the x rays, which are basically bremsstrahlung associated with the thermal motion of the particles, one can identify the K_α lines of the characteristic x rays (in particular, of highly ionized atoms with small and medium atomic number Z).[5–7] The discovery of characteristic x-ray radiation in the solar spectrum indicates the presence in the corona of high-energy particles, especially during the time of reduced activity of the Sun.[8] The changes in the intensities of the individual x-ray lines indicate changes in the fluxes of the high-energy particles.[9]

For cosmic objects far from the solar system it has not yet been possible to identify individual lines of x-ray transitions. However, in 1973 Serlemitsos *et al.*[10] reported the possible identification of x-ray transitions of the K series in the x-ray spectrum of the supernova Cas A.

To achieve optimal control of the processes in collective heavy-ion accelerators,[11] it is necessary to know the ionization cross sections of the atoms and ions for all ionization states. The diagnostics of the ions in the electron rings of such accelerators requires knowledge of the energy and intensity of the x-ray transitions that

 0090-4759/83/040349-28$04.40

take place when vacancies are formed in an inner atomic shell.[12] Nonradiative processes make an appreciable contribution to the formation of multiply charged ions due to filling of primary vacancies in inner atomic shells.[13-15]

Analysis of the x-ray spectra resulting from the irradiation of targets with ions also requires detailed knowledge of the influence of vacancies in the inner and outer shells.

Physical information about the ionization state, i.e., about the vacancy distribution in the shells, is contained in the transition energies of the characteristic x rays, in the energies of the emitted Auger electrons, and in the intensities of the corresponding x rays or the transition intensities of the Auger electrons. The binding energies of all electron states together with the excitation and ionization probabilities depend on the ionization state of the atom. On the basis of the change in the energy structure of the atomic shells one can formulate energy selection rules that preclude certain Auger or Coster–Kronig transitions in atoms in definite ionization states.

Nonradiative transitions significantly influence multiple ionization, i.e., the possibility of primary processes of the Auger or Coster–Kronig type determines the probability of the following cascades through the vacancies and, thus, the processes of many-electron emission. The shift in the balance between the radiative and nonradiative processes as the vacancy distribution in an atom changes is characterized by the fluorescence yield.

The development of powerful computers has made possible detailed calculations of atomic structures. There are programs that permit the solution of this problem by the self-consistent field method. These programs include approximations of different degrees of complexity: from calculations based on local potentials in the nonrelativistic[16] and relativistic[17-19] approximations to nonrelativistic[20,21] and relativistic[22-26] programs using nonlocal potentials and with inclusion of a Breit operator in the first order of perturbation theory to describe magnetic and retardation effects.[27,28]

To avoid the complexity of the solution of problems with a nonlocal potential, the averaged local Slater potential[29] is frequently used in various modifications. There are also programs that take into account quantum-electrodynamic effects (electron self-energy, vacuum polarization), which give additional corrections to the results of calculations with a self-consistent field.[30]

The above-mentioned programs provide a basis for constructing wave functions that can then be used to calculate the probabilities of radiative[31] and nonradiative[32] electron transitions in atomic shells and also ionization cross sections.[14,15,33]

The aim of the present paper is to discuss the most important processes in atomic shells associated with the occurrence of vacancies. We describe methods of calculating the parameters of atomic states and constructing wave functions for calculating the matrix elements of radiative and nonradiative transitions. We find the dependences of the energy and intensity of the characteristic x-ray radiation of ions on the ionization state. We discuss the change in the probability of nonradiative electron transitions with increasing ionization multiplicity, and we elucidate the part played by Auger and Coster–Kronig processes in the rearrangement of the shells. We give the cross sections of direct single and multiple ionization for ions of different charge states.

1. METHODS OF CALCULATING ATOMIC STRUCTURE

Basic problem

We describe here the most widely used methods of calculating atomic structure. To calculate the energy of an electron transition in atomic shells, it is necessary to determine the total energy of the atom for the initial and final electron states. The total energy E is found using the equation

$$H\Psi = E\Psi, \tag{1}$$

where H is the Hamiltonian operator, and Ψ is the many-particle wave function characterizing the considered electron state. This equation is usually called the *Schrödinger wave equation in the nonrelativistic case and the Dirac equation in the relativistic case*. For atoms possessing more than one electron, there is no exact solution of (1). Approximate solutions of the Schrödinger equation giving high accuracy in calculations have been found for the atoms of helium and its isoelectron sequence in Refs. 34 and 35. The most widely used method of approximate solution of problems for many-electron systems is the Hartree–Fock self-consistent field method.[36-39]

The self-consistent field method

General Principles. In the Hartree–Fock method, the potential and wave functions of the electrons are determined simultaneously in a self-consistent manner.[37-39] The Coulomb interaction potential $\sum_{i\neq j} 1/r_{ij}$ of the electrons together with the nuclear potential determines the total potential, for which the wave functions are calculated. The difficulties in the method are due to the fact that except for closed shells the total potential is noncentral. The wave function can be factorized into angular and radial parts only for a central potential. If the wave functions are factorized, the solutions are no longer exact solutions of the wave equation, and perturbation theory must be used to achieve the required accuracy of calculation.

The Hartree–Fock equations are obtained from the variational principle using the expression for the total energy of the atom

$$E = \langle \Psi \mid H \mid \Psi \rangle \tag{2}$$

and the normalization condition for the wave function. A complicating factor of the method is the need to take into account the Pauli principle, i.e., the antisymmetry of the wave function Ψ with respect to all pairs of electrons. The integro-differential equations derived from

the variational principle have the form

$$H_i\Psi_i = E\Psi_i + \sum_j C_{ij}\Psi_j,$$

where Ψ_i is the wave function of the ith electron. The exchange interaction (the second term) greatly complicates the solution of the Hartree–Fock equation.

In nonrelativistic calculations, it is necessary to solve N coupled equations, but in relativistic calculations one must solve $2N$ equations, since each wave function has two components. Although the Hartree–Fock method was developed about 50 years ago, the iterative solution of the corresponding nonlinear integro-differential equations on a large scale became possible only during the last two decades through the development of modern computational techniques. The Hartree–Fock method is expounded in detail in Refs. 37 and 38.

For a definite atomic configuration, the electron wave function $\Psi(1, 2, \ldots, N)$ is approximated by a determinant wave function, the antisymmetric product of single-electron wave functions Ψ_α corresponding to a central potential:

$$\Psi(1, 2, \ldots, N) = (N!)^{-1/2}\begin{vmatrix} \Psi_\alpha(1) & \Psi_\alpha(2) & \ldots & \Psi_\alpha(N) \\ \Psi_\beta(1) & \Psi_\beta(2) & \ldots & \Psi_\beta(N) \\ \vdots & \vdots & & \vdots \\ \Psi_\pi(1) & \Psi_\pi(2) & & \Psi_\pi(N) \end{vmatrix}. \quad (3)$$

Using a Hamiltonian that includes single- and two-particle operators, the total energy of the system can be expressed as follows:

$$E = \frac{\langle\Psi \mid H \mid \Psi\rangle}{\langle\Psi \mid \Psi\rangle} = \sum_\alpha I_\alpha + \frac{1}{2}\sum_{\alpha,\beta}(I_{\alpha,\beta} - K_{\alpha,\beta}), \quad (4)$$

where all the orbitals α and β of the individual configurations are taken into account; I_α characterizes the single-electron contributions and $I_{\alpha,\beta}$ and $K_{\alpha,\beta}$ the two-electron contributions. The single-electron wave functions can be found from the variational principle, which requires the total energy of the system to be minimal.

The wave functions in the central field are expressed in the form of products of the radial and angular single-electron wave functions:

$$\Psi_\alpha(i) = \Psi_{n_i l_i m_i}(r, \vartheta, \varphi)\chi_{s_i}(s) = \frac{1}{r}P_{n_i l_i}(r)Y_{l_i m_i}(\vartheta, \varphi)\chi_{s_i}(s), \quad (5)$$

where $P_{n_i l_i}$ is a radial wave function, dependently on only the quantum numbers n_i and l_i; $Y_{l_i m_i}$ are spherical harmonics, and $\chi_{s_i}(s)$ are spin functions. The factorization of the wave functions makes it possible to reduce the problem to the solution of a system of nonlinear integro-differential equations, the so-called Hartree–Fock equations, which are solved by numerical or analytic methods.

For atoms with incomplete shells, the many-electron wave function is represented as a linear combination of determinant functions that contain different incomplete sets of single-electron wave functions for a closed subshell or subshells. The structure of the Hartree–Fock equations depends on the particular form of the Hamiltonian and the single-electron wave functions.

Nonrelativistic Theory. The spin-independent nonrelativistic Hamiltonian of the many-electron system has the general form

$$H^{NR} = -\frac{1}{2}\sum_j \nabla_j^2 - \sum_j \frac{Z}{r_j} + \sum_{i>j}\frac{1}{r_{ij}}. \quad (6)$$

The first term in (6) is the kinetic-energy operator of the electrons, the second is the potential-energy operator of the electrons in the field of the nucleus with charge Z, and the third is the potential-energy operator of the Coulomb interaction between the electron pairs. Substituting (5) and (6) in (4), we obtain for the total energy of the system the expression

$$E = \sum_a q_a I(a) + \sum_{a\leqslant b}\sum_k A_{abk}F^k(a, b) - \sum_{a<b}\sum_k B_{abk}G^k(a, b), \quad (7)$$

where a and b are taken for all subshells of the atom. In the nonrealtivistic case, a and b depend on the quantum numbers n and l. The subshells a and b are characterized by the sets of quantum numbers $n_i l_i$ and $n_j l_j$. The single-electron contribution is described by $I(a)$, and it takes into account the kinetic energy of the electron in subshell a and its electrostatic interaction with the nucleus. The quantities $F^k(a, b)$ and $G^k(a, b)$ are the Coulomb and exchange integrals in subshells a and b. The two-electron integrals $F^k(n_i l_i, n_j l_j)$ and $G^k(n_i l_i, n_j l_j)$ are usually called *Slater integrals*. In (7), q_a, A_{abk}, and B_{abk} are the corresponding numerical coefficients. Slater proved that the expression (7) is also valid for atoms with partly filled electron shells. The values of the numerical coefficients for the different terms or LS multiplets are given in Ref. 38. In Appendix 21 of Ref. 38 there are tables for all possible multiplets associated with definite electron configurations and the corresponding coefficients of the coupling between the electrons and the partly filled subshells.

Nonrelativistic Hartree–Fock calculations make it possible to determine the energies of all multiplets. For many problems (for example, to calculate the energies of x-ray transitions and Auger transitions) it is sufficient to know the averaged (over LS) energy of the configuration.

A method of numerical solution of the radial Hartree–Fock equations was developed by Hartree.[37] There currently exist several programs for computer calculation of atomic structures, for example, the Froese,[40] Froese-Fischer,[21] and Mayers–O'Brien[41] programs. There is also an analytic approximate method based on work of Roothaan[42,43] in which the atomic orbitals are represented as linear combinations of basis functions of Slater or Gauss type.[44–46] Analytic calculations are difficult because of the necessity of nonlinear optimization of exponentials for the basis functions.

Molecular systems have lower symmetry than atoms or ions, and therefore factorization of the wave function in accordance with (5) becomes impossible. In this connection, it is necessary to perform a lengthy three-dimensional numerical integration, and therefore Roothaan's method is used for the majority of molecular calculations.

Relativistic Corrections to Nonrelativistic Hartree–Fock Calculations. By means of the Breit–Pauli effective Hamiltonian we introduce relativistic corrections:

$$H^{BP} = H^{NR} + H^{RC}.$$

The relativistic correction factor H^{RC} can be interpreted as the first term in the expansion of the energy of the N-electron system with respect to the parameter $1/c^2$ ($\equiv \alpha^2$ in atomic mass units, where α is the fine-structure constant). The correction H^{RC} has the form[47]

$$H^{RC} = \sum_{i=1}^{N} [f_i(so) + f_i(mass) + f_i(d)] + \sum_{i<j} [g_{ij}(so+so') + g_{ij}(ss') + g_{ij}(css') + g_{ij}(d) + g_{ij}(oo')]. \quad (8)$$

The single-particle operators in (8) are as follows:

$f_i(so) = \frac{\alpha^2 Z}{r_i^3}\mathbf{l}_i\mathbf{s}_i$, the spin-orbit interaction,

$f_i(mass) = -\frac{1}{4}\alpha^2\mathbf{p}_i^4$, the relativistic correction to the mass,

$f_i(d) = -\frac{1}{4}\alpha^2 Z\nabla_i^2\left(\frac{1}{r_i}\right)$, the Darwin correction.

The two-particle operators can be divided into two types:

a) the fine-structure operators $g_{ij}(so+so') = -\alpha^2[\mathbf{r}_{ij}/r_{ij}^3 \times \mathbf{p}_i(\mathbf{s}_i + 2\mathbf{s}_j) + \mathbf{r}_{ij}/r_{ij}^3 \times \mathbf{p}_j(\mathbf{s}_j + 2\mathbf{s}_i)]$, which describe the spin–orbit interaction plus the interaction of the spin with the orbital angular momenta of other orbits, and $g_{ij}(ss') = 2\alpha^2/r_{ij}^3[\mathbf{s}_i\mathbf{s}_j - 3(\mathbf{s}_i\mathbf{r}_{ij})(\mathbf{s}_j\mathbf{r}_{ij})/r_{ij}^2]$, which describe the spin–spin interaction;

b) operators not associated with the fine structure, namely, $g_{ij}(css') = -(16\pi/3)\alpha^2\mathbf{s}_i\mathbf{s}_j\delta^3(r_{ij})$, the spin–spin contact interaction; $g_{ij}(d) = (1/2)\alpha^2\nabla_i^2(1/r_{ij})$, the Darwin operator; and

$$g_{ij}(oo') = -\frac{\alpha^2}{r_{ij}}\left[\mathbf{p}_i\mathbf{p}_j + \frac{\mathbf{r}_{ij}(\mathbf{r}_{ij}\mathbf{p}_j)\,\mathbf{p}_i}{r_{ij}^2}\right]$$

the orbital interaction. Here, $\mathbf{r}_{ij}$ characterizes the spatial vector of the relative position of particles i and j, and $\mathbf{p}_i$ and $\mathbf{s}_i$ are the linear momentum and spin operators of particle i.

The influence of these interactions on the LS-coupled functions of the configuration states and on the functions of the atomic states depends on whether or not these operators commute with the total spin operators $\mathbf{S}^2$ and $\mathbf{S}_z$ and with the operators of the total angular momentum.

The single-particle corrections to the energy in Breit–Pauli perturbation theory increase for hydrogen-like atoms as α^2Z^4, while the two-particle corrections increase as α^2Z^3, i.e., these corrections increase rapidly compared with the nonrelativistic energy $[O(Z^2)]$ with increasing Z.[48] Allowance for the fine-structure operators improves the agreement between the calculations and the experimental data for light atoms and their ions. With increasing contributions from the fine-structure terms, the spectrum becomes sensitive to the splitting of the terms,[47] and neglect of the terms not associated with the fine structure, which influence the term splitting, the total energy, and the ionization potentials, can lead to a loss of accuracy of the calculations.

Intermediate Type of Coupling. In nonrelativistic calculations, the spin–orbit interaction, which lifts the degeneracy of the J states, is taken into account by the corrections to the energies of the LS multiplets. A detailed description of the method is given in Ref. 49. The splitting of the levels depends on the spin–orbit coupling coefficient K_{SB}, which in the approximation of a central field has in atomic units the form

$$K_{SB} = \int_0^\infty P_{nl}^2(r)\,\xi(r)\,dr = \frac{\alpha^2}{2}\int_0^\infty P_{nl}^2(r)\left[\frac{1}{r}\frac{\partial V}{\partial r}\right]dr, \quad (9)$$

where $V(r)$ is the potential energy of an electron in the self-consistent field. A method of calculating the coupling coefficients is given in Ref. 50.

In an alternative approach, the coefficients K_{SB} are determined from the known binding energies E_{nl}^Z of individual subshells:

$$K_{SB} = \frac{2}{2l+1}[E_{nl}^Z(^2L_{l-1/2}) - E_{nl}^Z(^2L_{l+1/2})].$$

The intermediate-coupling technique is widely used in the interpretation of x-ray spectra and the spectra of Auger electrons. This model describes very well vector coupling for many atoms.[51]

Relativistic Theory. The Breit–Pauli approximation is not suitable for atoms with high Z, since perturbation theory does not hold for them. Therefore, it is desirable to use a theory in which the single-electron terms are calculated without perturbation theory. This can be achieved by using the single-electron orbitals obtained by solving the Dirac equation.

A relativistic variant of a Hartree–Fock-type equation for a many-electron system was first formulated by Swirles.[52,53] The many-electron wave function Ψ is approximated by a linear combination of determinant functions. The employed single-electron central-field wave functions are the relativistic functions obtained by Dirac[54,55] and Darwin.[56] For the solution of particular problems, the relativistic equations of Hartree–Fock type (the Dirac–Fock equations) were reformulated by Grant[57] using the algebra of tensor operators. A detailed description of the relativistic theory was given by Grant.[39]

The relativistic Hamiltonian for the many-electron system has the form

$$H^R = \sum_{i=1}^{N} h_D(i) + \sum_{i<j} g(i,\ j), \quad (10)$$

where $h_D(i) = -ic\alpha_i\nabla_i + \beta_i c^2 + V(r_i)$ is the Hamiltonian of electron i moving in the Coulomb field of the nucleus with charge Z. This Hamiltonian takes into account the relativistic variation of the mass and the spin–orbit interaction of the electrons; α and β are Dirac operators[39]; $V(r_i)$ is the potential energy of the interaction of electron i with the nucleus. For small and medium Z, the nucleus is regarded as a point and the potential is $V(r_i) = -Z/r_i$. For atoms with large Z ($Z \geq 80$), the potential $V(r_i)$ is described by a more complicated function, which takes into account the finite radius of the nucleus.[39]

The functions $g(i,j)$ are related to the interaction energy of electron pairs:

$$g(i,\ j) = 1/r_{ij} + B(i,\ j). \quad (11)$$

The first term in (11) describes the Coulomb interac-

tion of the electrons. The Breit operator[18] is

$$B(i,\ j) = -\alpha_1 \cdot \alpha_2 \cos(E_\omega r_{ij})/r_{ij} + (\alpha_1 \nabla_1)(\alpha_2 \nabla_2)[\cos(E_\omega r_{ij} - 1)/E_\omega^2 r_{ij}]$$
$$= -\alpha_1 \alpha_2 / r_{ij} - (1/2r_{ij})(\alpha_1 \nabla_1)(\alpha_2 \nabla_2) + O(E_\omega^2 r_{ij}),$$

where E_ω is the exchange energy of the electrons. The Breit operator takes into account magnetic and retardation effects, which in the nonrelativistic approximation correspond to orbital interaction and the spin–spin contact interaction. Usually, the contributions from the magnetic and retardation effects are taken into account in the first order of perturbation theory. When the relativistic Hamiltonian (10) is used, the single-particle interactions are taken into account in $h_D(i)$, the Coulomb interaction of the electrons by the term $1/r_{ij}$, and all the remaining corrections are included in the Breit operator.[48] On the basis of a relativistic approximation of Dirac–Fock type, programs have been developed for computer calculations with allowance for the exchange interaction.[22–28] The retardation, magnetic, and correlation effects are not taken into account. Their contributions can be partly estimated by perturbation theory. A relativistic generalization of the Hartree–Fock–Roothaan equation is given in Refs. 58 and 59, in which analytic approximations are obtained for the single-electron wave functions.

Slater Exchange Potential. In the Hartree–Fock equations, the exchange potential is nonlocal, which greatly complicates their solution. Numerical calculations are very complicated and require much computer time even with modern computers.

To simplify the Hartree–Fock equations, Slater proposed that the intractable exchange terms should be replaced by an average exchange potential.[29] The resulting equations are usually called the Hartree–Fock–Slater equations. The solution of these equations requires much less computing time. The Slater exchange potential is obtained by averaging the potential of the electrons over all occupied electron states with definite weight factors and by multiplying by the density of electrons at the point **r**.

This method gives the average density of the exchange potential and, accordingly, a common average exchange potential $V_A(r)$ for all states. This potential is usually parametrized in the general form[26]

$$V_A(r) = -\frac{C}{r}\left(\frac{81}{32\pi^2} r^n \rho(r)^m\right)^{1/3},$$

where $\rho(r)$ describes the radial charge density, and C, m, and n are constants. In his original paper,[29] Slater chose $C = m = n = 1$. The use of wave functions calculated by means of the Slater exchange potential leads to results intermediate between the Hartree and Hartree–Fock models. The energy eigenvalues of individual electron states in Hartree–Fock–Slater calculations differ little from the Hartree–Fock results, since inaccuracy in the wave function gives an error in the energy eigenvalue in the second order.[29]

To obtain better agreement with the experimental data, the Slater potential was modified. Several modified potentials[18,60–64] give better agreement between the calculated and experimental results. The Kohn–Sham–Gáspár approximation[60,63] with $C = 2/3$ and $m = n = 1$ is widely used.

The X_α method[64,65] is based on the introduction of a parameter α in the Slater exchange potential,

$$V_{X_\alpha}(r) = \alpha V_A(r),$$

which is done to make the energy eigenvalues calculated in the Hartree–Fock model using the true exchange potential equal to the eigenvalues calculated in the model with the Slater exchange potential. The choice of the parameter α has been discussed in particular by Gopinathan *et al.*[66] Naturally, one cannot expect the Hartree–Fock equations modified in this manner to give wave functions satisfying the original equations. However, the relative simplicity of solution of the equations with the Slater exchange potential justifies its use in many cases (see Refs. 18, 26, and 67–71).

In the Hartree–Fock model, the Coulomb interaction potential of the electrons is partly compensated by the exchange potential, in contrast to the Hartree–Fock–Slater model, in which the interaction potential at large distances from the nucleus differs from the real potential. To correct this defect in the potential of the atom, Latter[72] proposed a correction method in which the potential has the form

$$V(r) = V_0(r) \text{ for } r < r_0;$$
$$V(r) = -2(Z - I + 1)/r \text{ for } r \geqslant r_0.$$

The distance r_0 is determined from the condition

$$V_0(r_0) = -2(Z - I + 1)/r_0,$$

where I denotes the number of vacancies in the atom, and $V_0(r)$ is the sum of the potential of the nucleus, the Coulomb potential of the electrons, and the exchange potential.

In the nonrelativistic approach, the program developed by Herman and Skillman[16] was mainly used for computer calculations of atomic structure. They used the wave functions of the nonrelativistic program in the Hartree–Fock–Slater model to estimate in the first order of perturbation theory the contributions of the relativistic corrections and the spin–orbit interaction. The relativistic calculations by the Dirac–Fock–Slater method were made by Rosén and Lindgren,[18] Liberman *et al.*,[17,67] and Lu *et al.*[19] The energies and single-electron wave functions calculated in this way have been used in many studies to determine the transition energies of the satellites of x-ray lines and Auger electrons and to calculate the transition matrix elements of electrons in radiative and nonradiative processes. Huang *et al.*[73] used Dirac–Fock–Slater wave functions to calculate the binding energies of electrons for neutral atoms with inclusion of the magnetic and retardation effects, and also the quantum-electrodynamic corrections (vacuum polarization, electron self-energy).

Hartree Method. For completeness of the exposition, we briefly characterize the point of departure of all self-consistent calculations. The Hartree method is a simplified form of the radial Hartree–Fock equations obtained by ignoring completely in them the exchange interaction. The many-electron wave function

$\Psi(1,2,\ldots,N)$ (see above) is replaced by a simple product of single-electron wave functions:

$$\Psi(1,\ 2,\ \ldots,\ N)=\Psi_\alpha(1)\,\Psi_\beta(2)\ \ldots\ \Psi_\pi(N).$$

This simple procedure was widely used prior to the advent of powerful computers, which made it possible to overcome the barrier of long computing times associated with the solution of the Hartree–Fock equations.[37,74,75] At the present time, such calculations are not as a rule made because their results in the majority of cases deviate much more strongly from the experimental results than do calculations by the Hartree–Fock or Hartree–Fock–Slater methods.

Comparison of Methods of Calculating Atomic Structure. Many calculations of atomic structure using different approximations have been made. Because of the large number of such calculations, it is impossible to discuss the results of each paper separately. However, in the literature one can trace certain general directions characteristic of the models discussed above.

Two main directions are the relativistic and nonrelativistic methods. In the original nonrelativistic calculations, the total energy of the system is minimized for the Hamiltonian associated with the Schrödinger equation. Correlation effects influence the results of the calculations even at low Z, and it is recommended that they always be taken into account. In the first order of perturbation theory, relativity is taken into account by adding corresponding terms to the effective Breit–Pauli Hamiltonian using nonrelativistic wave functions. An improved description of the most important relativistic effects associated with the motion of the electrons is achieved by using the Dirac single-electron Hamiltonian and the development of a theory analogous to the nonrelativistic theory. The interaction of electron pairs is taken into account, as in the nonrelativistic theory, by the Coulomb field. Retardation effects, the higher quantum-electrodynamic corrections, and the electron correlation effects are taken into account, depending on the particular problem.

Table I gives the experimental values of level energies, which are compared with calculated energies obtained in various ways. As a rule, the calculations without allowance for the relativistic effects differ more strongly from the experimental data than do the relativistic results. In relativistic calculations, the relativistic effects influence the electrons of the outer shells indirectly through the increase in the binding energy of electrons with small angular momentum.[67,78] In the relativistic theory, the electron orbitals with small angular momenta approach the nucleus and screen the electrons with higher angular momenta more effectively. This leads to a decrease in the binding energy of the electrons if the exchange effects do not have the opposite influence. Very good agreement between the calculated and experimental electron binding energies was obtained by Huang *et al.*[73] in the adiabatic approximation of the Dirac–Fock–Slater method with allowance for magnetic, retardation, and quantum-electrodynamic effects.

We give an idea of the individual contributions to the total energy (atomic units) for the example of the binding energy of an electron in the K shell of mercury ($Z = 80$)[39]:

TABLE I. Comparison of experimental and calculated electron energy levels. All energies are given in atomic units (1 a.u. = 27.2116 eV).

Orbital	Herman and Skillman		Fraga *et al.*	Rosén and Lindgren		Huang *et al.*		Liberman *et al.*	Desclaux	Experiment
	A	B		A	B	A	B			
Argon										
$Z=18$										
1s 1/2	116.268	116,926	118.610	119,070	117.928	117,918	117,795	116.776	119,427	117.703±0.011
2p 3/2		9,123		9,519	9,118	9,110	9,106	9.080	9.547	9,011±0,011
3s 1/2	1.053	1,069	1.280	1,283	1.225	1,226	1.220	1,063	1.287	0,930±0.015
3p 3/2	0.533	0,535	0.590	0.584	0,537	0,536	0.536	0,530	0.588	0.456±0.011
Krypton										
$Z=36$										
1s 1/2	515.320	526,125	520.150	529,650	527.680	527,670	526.460	526,539	529.690	526.452±0.029
2s 1/2	67.628	70,477	69.900	72,010	71,050	71,050	70,950	70,523	72.080	70.595±0.022
2p 3/2	61,624	62,082	63.000	62.820	61,770	61,770	61,770	61,530	62,880	61,551±0.018
3p 3/2	7,624	7,742	8.330	8,295	7,974	7,974	7,968	7,616	8.313	7,857±0.040
3d 5/2	3.549	3,571	3,830	3,711	3,380	3.382	3,383	3,057	3.727	3,234±0.029
4s 1/2	0,973	1.036	1,150	1,197	1,136	1,132	1,132	0,983	1.188	0.882±0.029
Uranium										
$Z=92$										
1s 1/2	3704.600	4243,150	3717,550	4286,060	—	4275,290	4248,110	4272,646	4279,230	4248,412±0,059
2p 3/2	624,770	649,620	629.800	635,550	—	633,170	631,020	631,364	635,570	630,845±0,011
3s 1/2	163,318	200,138	167,450	206,890	—	205,210	204,910	203,155	204,395	203.884±0.015
3d 5/2	134,404	137,458	136,960	132,420	—	130,980	130,760	130,601	132,420	130,521±0,011
4d 5/2	28,154	29,260	30.040	28,140	—	27,500	27,480	26,983	28,130	27,110±0,011
4f 7/2	15,977	16,278	17,190	14,790	—	14,140	14,150	14,323	14,790	14,000±0,033
5s 1/2	9,245	11,955	10,840	12,620	—	12,270	12,260	11,792	12,600	11,896±0,040
5d 5/2	4,219	4,463	5,230	4,005	—	3,751	3,751	3,802	4,042	3,539±0,051
6s 1/2	1,482	2,018	2,450	2,161	—	2,027	2,026	1,915	2,138	2,598±0,044
6d 3/2	0,225	0,275	—	0,206	—	0,182	0,182	0,169	0,193	—

Note. Herman and Skillman[16]: A are the energy eigenvalues found by the Hartree–Fock–Slater (HFS) method with frozen orbitals (FO), and B is A +relativistic corrections (single-particle terms); Fraga *et al.*[20]: eignevalues by the HFS method with FO; Rosén and Lindgren[18]: A are the eigenvalues by the Dirac–Fock–Slater (DFS) method with FO, and B are the binding energies by the DFS method in the adiabatic approximation (AP); Huang *et al.*[73]: A are the eigenvalues by the DFS method in the AP, and B are the eigenvalues by the DFS method in the AP with allowance for the Breit operator and the quantum-electrodynamic corrections; Liberman *et al.*[17]: eigenvalues by the DFS method with FO; Desclaux[76]: eigenvalues by the DF method with FO; the experimental values are from Ref. 77.

Electrostatic interaction	3070.825
Magnetic interaction	12.045
Quantum-electrodynamic correction to the self-energy	7.325
Vacuum polarization	1.645
Retardation effects	0.885
Correlation interaction	0.040
	3092.765

In calculations of the structure of the atomic shells of heavy elements, the finite size of the nucleus becomes particularly important. The correction associated with the finite volume of the nucleus increases with increasing Z. This correction is less than 0.1% for $Z = 80$, is about 1% for $Z = 114$, and about 4% (around 10 keV) for the K shell of element $Z = 126$.[79] The probability of an electron of the K shell being within the nucleus is 0.0014% for $Z = 79$, but it is already 0.0058% for $Z = 92$.[39]

For many problems, it is not necessary to calculate the absolute values of the atomic-structure parameters; only their relative changes are needed. Such problems can be solved using truncated programs which ignore definite types of interaction or take them into account only in averaged form (see the Slater potential).[80] This is very important, since the relativistic computational programs of Hartree–Fock type on an EC-1060 computer consist of approximately 4500 (for multiconfiguration programs more than 10 000 (Ref. 28)) charts[37] and require a computer memory of approximately 350 kbytes to calculate 40 orbitals with integration over 250 points. To make calculations for very high Z, it is necessary to raise the number of points of integration for each orbital to 400, and the memory requirement increases to 500 kbytes. The characteristic times required for the calculation of one configuration range from a few minutes to tens of minutes. Programs with reduced number of interactions require, as a rule, much less computing time and much smaller memory.

2. CHARACTERISTIC x-RAY RADIATION

Calculation of x-ray transition energies

Among the radiative transitions in atomic shells, characteristic x-ray transitions are the most important. They take place when a vacancy is formed as a result of ionization in the inner electron shells of an atom. The vacancy is filled by an electron from the outer shells. The electrons of the outer shells have lower binding energy than those of the inner, and the difference between the binding energies in the electron transition is equal to the x-ray energy. The discrete nature of the energies of the electron levels leads to discrete x-ray transitions. The x-ray lines formed in this manner in a neutral atom are called *diagram* lines; in a multiply ionized atom, *nondiagram* lines. Diagram lines are systematized in Ref. 81.

The energy of transitions in atoms or ions associated with de-excitation processes can be calculated if one knows the total energies of the initial and final state of the electrons:

$$E^Z_{\text{(transition)}} = E^Z_{\substack{\text{total}\\ \text{(initial state)}}} - E^Z_{\substack{\text{total}\\ \text{(final state)}}}$$

The energy of an x-ray transition in an atom with atomic number Z from subshell (n,l,j) to subshell (n',l',j') is equal to the difference between the binding energies $\varepsilon^Z_B(n,l,j)$ and $\varepsilon^Z_B(n',l',j')$ of the subshells:

$$E^Z((n,\ l,\ j)\to(n',\ l',\ j')) = \varepsilon^Z_B(n',\ l',\ j') - \varepsilon^Z_B(n,\ l,\ j).$$

The binding energy $\varepsilon^Z_B(n,l,j)$ of the electron in subshell (nlj) is calculated as the difference between the total energies of the corresponding initial and final states of the atom. The initial state contains the considered electron, and in the final state it is gone:

$$\varepsilon^Z_B(n,\ l,\ j) = E^Z_{\substack{\text{total}\\ \text{(initial config)}}} - E^Z_{\substack{\text{total}\\ \text{(final config.)}}}. \qquad (12)$$

In self-consistent field calculations, the exact transition energy E^Z (transition) can be represented as a sum of several individual contributions:

$$E^Z_{\text{(transition)}} = E^{\text{NR}}_{\substack{\text{HFS}\\ \text{(transition)}}} + E_{\substack{\text{A}\\ \text{(transition)}}} + E_{\substack{\text{rel}\\ \text{(transition)}}} + E_{\substack{\text{cor}\\ \text{(transition)}}} + E_{\substack{\text{QED}\\ \text{(transition)}}}, \qquad (13)$$

where $E^{\text{NR}}_{\text{HFS}}$ (transition) is the difference between the total energies in the nonrelativistic Hartree–Fock–Slater calculation, E_{A} (transition) is the difference between the exchange energies, E_{rel} (transition) is the difference between the relativistic contributions to the energy, E_{cor} (transition) is the difference between the correlation energies, and E_{QED} (transition) is the difference between the contributions of the quantum-electrodynamic corrections. The choice of the method of calculation determines what terms in (13) are taken into account. In self-consistent Dirac–Fock calculations, the contributions E_{cor} and E_{QED} are ignored; in Hartree–Fock calculations, the contributions E_{rel}, E_{cor}, and E_{QED}; and in Hartree–Fock–Slater calculations, E_{A}, E_{cor}, E_{rel}, and E_{QED}. To take into account E_{cor}, multiconfiguration programs are used,[21,27,28] and to take into account E_{QED} additional programs by means of which the corresponding corrections are calculated using the wave functions from the programs we have mentioned.[30]

In many cases, especially for the outer shells, Hartree–Fock calculations give results in better agreement with the experiments than Dirac–Fock calculations. The Hartree–Fock method gives a good accuracy of calculations of the energy shifts of the x-ray lines relative to the diagram lines in the presence of additional vacancies.[82] For successful use of the truncated methods of description the difference between the ignored contributions to the transition energy must be small.

The electron binding energies are determined in two ways with allowance for the relaxation time of the electron states. If a transition or ionization process takes place so rapidly that the other electrons of the systems do not succeed in following the change of the electron configuration, a single set of radial wave functions is used to describe the initial and final states of the electrons. Koopmans[83] showed that in such a model, which is called the *frozen-orbital method*, the binding energy of an electron in the orbital (n,l,j) is

$$E^Z_B(n,\ l,\ j) = -\varepsilon_{nlj}\ \text{(Koopmans's theorem)}, \qquad (14)$$

where ε_{nlj} is the single-electron energy eigenvalue obtained by solving the Hartree–Fock equations for the

original atom. We note that Koopman's theorem does not hold in multiconfiguration calculations or in calculations using the Slater exchange potential. However, it is standard practice to compare the eigenvalues obtained in such calculations with the experimentally measured level energies.[39] To calculate the relaxation effects, the expression (14) is replaced by

$$E_B^Z(nlj) = -\varepsilon_{nlj} - \delta\varepsilon_{nlj},$$

where $\delta\varepsilon_{nlj}$ describes the correction associated with the contribution of the exchange interaction of the electrons.

The *adiabatic approximation* is an alternative to the frozen-orbital method. It is assumed that the electrons have sufficient time to redistribute themselves during the ionization process. The transition energy is calculated as the difference between the total energies of the corresponding states of the atom and the ion, i.e., different radial wave functions are used to describe the initial and final states. The energy of the true ground state of the ion is lower than in the frozen-orbital approximation, in which the total energy of the system is not minimized. The use of the adiabatic approximation is complicated by two factors that must be taken into account: 1) the transition energy is the small difference of two large quantities, and therefore the error of the calculations increases; 2) for n binding energies, $n+1$ individual calculations are needed.

Systematic comparison of the experimental values of the transition energies with the values calculated in the two approximations shows that the adiabatic approximation gives better agreement for the inner shells but worsens the results for the optical shells.[18,39]

At the present time, there are no reasons justifying the exclusive use of a particular method in atomic-structure calculations. The accuracy of the calculation of the energies of x-ray transitions depends on the accuracy with which the corresponding electron binding energies are calculated. For light elements, the standard programs using the Hartree–Fock or Dirac–Fock methods give adiabatic energies that differ by only a few electron volts from the experimental values. For heavy elements, the calculation of the electron binding energies of the inner shells requires more accurate methods that take into account the electromagnetic corrections and the correlation and quantum-electrodynamic effects.

The binding energies for the K shell of elements with $70 \leq Z \leq 90$ can be calculated to an accuracy better than 10^{-4} (Ref. 84). The experimental energies of x-ray transitions with the participation of valence electrons are sensitive to the chemical conditions. The discrepancies between the calculated and experimental values can also be explained by the fact that, as a rule, the calculations are made for isolated atoms or ions.

Satellites of x-Ray Lines

General Comments. Additional vacancies in the atomic shells are formed as a result of photoionization, collisions of atoms with electrons, protons, or heavy ions, or as a result of internal nuclear transformations. The characteristic x-ray lines and the Auger emission lines that arise when inner vacancies are filled in multiply ionized atoms differ in energy from the corresponding diagram lines. It is characteristic that with increasing degree of ionization in a shell containing an inner vacancy the x-ray transition energy increases, while the energy of the Auger transitions decreases.[85-87] An exception to this general rule is observed only for intershell x-ray transitions.[88] The same physical picture is observed for hypersatellites with not one but two initial vacancies in one shell in the primary state of a multiply ionized configuration.

TABLE II. Influence of outer and inner vacancies on the energy shifts of the x-ray K_α emission of chlorine. For the inner vacancies ($1s^2 2s^2 2p^{6-n} 3s^2 3p^5$) the experimental values of Ref. 89 are given; for the outer ($1s^2 2s^2 2p^6 3s^2 3p^{5-n}$), the results of Dirac–Fock–Slater calculations.

Configuration, n	ΔE, eV	
	($1s^2 2s^2 2p^{6-n} 3s^2 3p^5$)	($1s^2 2s^2 2p^6 3s^2 3p^{5-n}$)
1	18.3±1.4	0.402
2	36.9±1.8	1.104
3	56.6±2.2	2.120
4	77.2±2.0	3.520
5	98.4±2.8	5.308

The energy shifts of the satellite lines are much weaker when there are outer instead of inner vacancies. This effect for the chlorine atom is demonstrated in Table II.

For greater clarity, we give once more the explanation for the difference between the diagram x-ray and Auger lines from the satellite lines.

1. A diagram x-ray line or an Auger line arises because of a transition in which the initial state corresponds to a singly ionized atom, i.e., one electron has been removed, and all the remainder are in their orbitals. The final state for an x-ray transition again corresponds to a singly ionized atom; for an Auger transition, to a doubly ionized atom.

2. All other vacancy configurations form satellite lines.

Influence of Outer Vacancies on the Energies of x-Ray Transitions. *Validity of atomic-structure calculations.* Outer vacancies play a particularly important part in the behavior of hot plasmas[2] and bunches of charged particles.[12] The existence of outer vacancies influences the characteristics of the structural processes and the interaction strengths, in particular the nucleus–atomic shell interaction.

Hitherto there have been hardly any experimental investigations of the energy shifts of individual characteristic x-ray lines of heavy ions. This is due to the limited number of suitable heavy-ion sources and the high requirements on the experimental technique and method. It is only possible to calculate the shifts of the characteristic x-ray lines by means of the methods described in Sec. 2.

Because of the absence of experimental results, a

TABLE III. Comparison of energy shifts of K_{α_1} line (eV) of lead ions relative to the diagram line obtained in different ways (I is the number of outer vacancies).

I	DF(a)	DF(f)	DFS(f)	HFS	DFS(a)	DFS(ts 1)	DFS(ts 2)	DFS(K-1)
1	0.082	0.015	0.059	0.053	−0.082	0.078	0.078	0.090
2	0.191	0.094	0.151	0.144	0.000	0.194	0.191	0.213
4	0.517	0.312	0.451	0.397	0.585	0.535	0.522	0.541
10	0.245	0.135	0.093	0.010	0.013	−0.054	−0.052	0.041
12	0.109	0.165	0.157	0.150	−0.082	−0.141	−0.133	0.022
14	−0.271	−0.040	−0.182	0.136	−0.205	−0.204	−0.189	0.048
22	12,318	10,676	11,240	11,386	11,498	11,578	11,384	11,671
54	80,102	73,774	71,810	74,830	72,598	72,514	71,376	72,746
60	128,201	123,459	102,232	115,098	98,378	98,364	97,119	104,914
64	158,165	154,989	138,033	161,989	129,718	129,750	128,459	142,370
68	290,770	280,452	256,909	287,015	248,768	248,835	246,307	261,444
70	387,023	363,856	343,641	375,759	336,718	336,878	332,891	346,969

Note:

DF(a): adiabatic calculations by the Dirac–Fock method with allowance for magnetic and retardation effects.

DF(f): calculations by the Dirac–Fock method with allowance for magnetic and retardation effects for frozen orbitals.

DFS(f): calculations by the Dirac–Fock–Slater method (exchange potential with $C=m=n=1$) with Latter's modified Coulomb potential (see Sec. 2) for frozen orbitals.

HFS: calculations by the Hartree–Fock–Slater method using free-electron exchange potential.[90,91]

DFS(a): adiabatic calculations by the Dirac–Fock–Slater method.

DFS(ts 1): calculations of transition state by the Dirac–Fock–Slater method. In these calculations, the relaxation of the primary vacancy is taken into account approximately. It is assumed that the initial and final state of the x-ray transition have half vacancies. The x-ray transition energy is determined as the difference between the energy eigenvalues for the initial and final states. The modified Kohn–Sham potential[91] is used to calculate the energy eigenvalues.

DFS(ts 2): calculations of the transition state by the Dirac–Fock–Slater method. The energies of the x-ray transitions are determined as the differences of the corresponding electron binding energies. These energies are calculated as the differences of the total energies of the considered ion and the ion with one less electron in the considered subshell. In all calculations, the wave functions of the initial ion were used.

DFS($K-1$): calculations by the Dirac–Fock–Slater method with frozen orbitals. Besides a definite number of outer vacancies, an additional vacancy in the K shell was taken into account in the calculation.

problem arises: Which of the methods of calculation described in Sec. 2 describe the physical situation best? In calculations of x-ray transition energies it is not the absolute values for different degrees of ionization of the atom that are of primary interest but rather the relative shifts.

The shifts of the energy of the K_{α_1} line of lead ions relative to the energy of the diagram line is given in Table III.

In comparing the results in Table III, it can be assumed that the best agreement with physical reality is achieved in adiabatic calculations by the Dirac–Fock method [DF(a)] using Desclaux's program.[27] It can be seen from Table III that when electrons are removed from the outer shells ($6s$, $6p$) calculations of the transition state by the Dirac–Fock–Slater method [DFS (ts 1, 2)] agree satisfactorily with the adiabatic Dirac–Fock calculations [DF (a)]. As more inner electrons are removed ($n \leq 5$), the agreement between the Dirac–Fock–Slater calculations using a free-electron exchange potential (HFS) and Dirac–Fock calculations [DF (a)] improves. At low degrees of ionization, the nature of the change in the shifts is correctly reflected. All the remaining methods of calculation at high degrees of ionization give energy shifts of the x-ray transitions that are too low.

The calculated energy shifts of the x-ray K_{α_1} transition for lead ions are given in Fig. 1. The shifts of the K_{α_1} line for the ground states of the lead ions found by the Dirac–Fock–Slater method using the free-electron exchange potential[90,91] for frozen orbitals are compared with the shifts of the K_{α_1} line obtained in adiabatic calculations by the Dirac–Fock and Dirac–Fock–Slater methods. As follows from Table III and Fig. 1, all the methods of calculation give, apart from model deviations, similar behavior of the shifts of the x-ray transition energies with increasing number of vacancies in the outer shells. A similar behavior of the energy shifts of the x-ray lines for lead was found by Arndt *et al.*[80] in adiabatic calculations by the Dirac–Fock method and calculations with various local potentials. McGilp and Weightman[93] also point out that the choice of the particular method of calculation in the framework of central-field approximations does not lead to results differing strongly from each other in an analysis of the dependence of the internal properties of the atomic shell on the degree of ionization of the atom. It is much more important in the various calculations to take into account the same corrections to the Hamiltonian that describes the particular system. The electron binding energies for zinc, cadmium, and mercury calculated in Ref. 93 by two different methods in the

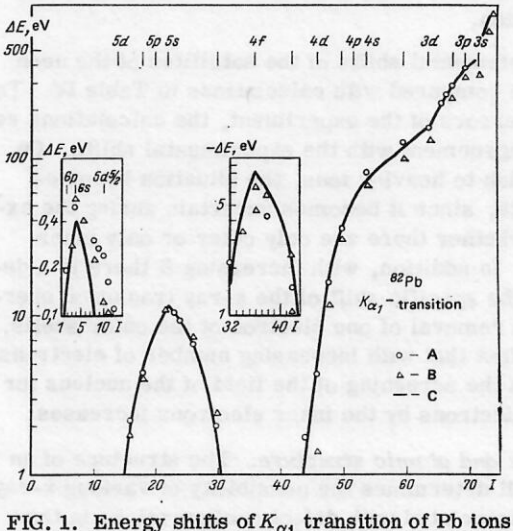

FIG. 1. Energy shifts of K_{α_1} transition of Pb ions obtained from adiabatic calculations by the Dirac–Fock and Dirac–Fock–Slater methods and by the Dirac–Fock–Slater method with frozen orbitals: A) adiabatic calculations by the Dirac–Fock method; B) adiabatic calculations by the Dirac–Fock–Slater method; C) calculations with frozen orbitals by the Dirac–Fock–Slater method. I is the number of outer vacancies.

central-field approximation agree well, although the energies were determined by means of two very different programs. The electron binding energies were determined in the adiabatic approximations by the Dirac–Fock method[27] and by the Dirac–Fock–Slater method.[73]

The excellent agreement between the two methods, which take into account the exchange interaction between the electrons in different ways, show that both methods give a good approximate solution of the problem. In addition, the good agreement for the electron binding energies calculated in the adiabatic approximation indicates that the two methods are equally suitable for calculating ionized states of the atom, since the total energy of the singly ionized atom enters into the adiabatic calculation of the electron binding energies. It can be concluded from the results we have given that the Dirac–Fock–Slater method makes it possible to calculate the atomic structure of highly ionized atoms rather accurately. The use of a local rather than a nonlocal exchange potential does not change the qualitative results and only slightly changes the quantitative results.

As we have already pointed out, not much is known about the influence of outer vacancies on the properties of atomic shells. We compare the experimental energy shifts of satellites with calculated data, using the known spectrum of the x-ray K satellites of neon. The atomic structure of neon ($1s^2 2s^2 2p^6$) is convenient for investigating the influence of outer vacancies. The physical picture in this case is fairly simple. At higher atomic numbers $Z > 10$, the experimental picture is complicated by the fact that, as a rule, pure configurations with outer or inner vacancies are not observed. In addition, neon is suitable for investigating the influence of outer vacancies because nonradiative transitions from the higher-lying principal shells or within a definite principal shell are impossible for it. Thus, the obtained experimental information admits unambiguous phyical interpretation.

The experimental shifts of the satellites of the neon K_α line are compared with calculations in Table IV. To within the errors of the experiment, the calculations reveal good agreement with the experimental shifts. On the transition to heavier ions, the situation becomes less definite, since it becomes uncertain during the experiment whether there are only outer or only inner vacancies. In addition, with increasing Z there is a decrease in the specific shift of the x-ray transition energies on the removal of one electron of the outer shells, due to the fact that with increasing number of electrons in the atom the screening of the field of the nucleus for the outer electrons by the inner electrons increases.

Satellites and atomic structure. The structure of an atomic shell determines the possibility of various x-ray satellites associated with defect configurations in the outer shells of the atom. Depending on the particular structure of the atomic shell, the number of x-ray transitions increases with increasing Z. However, some transitions are possible only for definite degrees of ionization and for distinguished vacancy configurations. The maximal degree of ionization at which a certain x-ray transition can still be observed can be represented as a function of the atomic number Z in the form

$$I_{\max}(Z) = Z - K(Z),$$

where $K(Z)$ is a constant for the considered type of transition.

TABLE IV. Influence of outer vacancies on the energies of x-ray K_α transitions of neon ions of $1s^1 2s^n 2p^m$ configurations.

Configuration n	m	Satellite	E_{exp}, eV	ΔE_{exp}, eV	E_{HF}, eV	E_{DFS}, eV
2	6	KL^0	848±2	—	—	—
2	5	KL^{-1}	855±2	7±4	6,1	5,8
1	6					
2	4	KL^{-2}	863±2	15±4	14,5	13,4
1	5					
0	6					
2	3	KL^{-3}	873±2	25±4	25,4	22,6
1	4					
0	5					
2	2	KL^{-4}	882±2	34±4	31,7	34,3
1	3					
0	4					
2	1	KL^{-5}	895±2	47±4	45,3	45,9
1	2					
0	3					
1	1	KL^{-6}	907±2	59±4	56,1	57,1
0	2					

Note. E_{exp} are the experimental values[94]; ΔE_{exp} are the experimental energy shifts of the satellites; E_{HF} are the results of Dirac–Fock–Slater calculations using a free-electron exchange potential without additional vacancy in the K shell; E_{DFS} are the results of Dirac–Fock–Slater calculations with the Slater exchange potential.

When electrons are knocked out of an atomic shell, various vacancy configurations are formed. In what follows, we shall consider only those processes in which a positive ion goes over to its ground state, which corresponds to the minimum of the total energy of the many-electron system. The ground-state configurations of ions calculated by the energy-minimization principle differ from the electron configurations of the neutral atoms with the same number of electrons. The localization of the vacancy in the ground state of an ion begins with the 7s and 6d orbitals[95] and is displaced in the sequence 5f, 6p, 6s, 5d, 4f, 5p, 5s, 4d, 4p, 4s, 3d, 3p, 3s, 2p, 2s, and 1s.

Irregular behavior in the filling of orbitals in the ground state begins with $Z = 57$. For all elements with $Z < 57$, electrons with the largest quantum numbers are the first to be removed from the ground state of the ion. The ionization takes place in such a way that the electron with the highest values of the quantum numbers n, l, j is always stripped.

However, there are a number of exceptions to this rule, for example, for $Z = 23, 27, 28, 39, 57, 58$. The change of the occupied electron orbitals in the ground state of the ion is shown for the first three degrees of ionization for all elements up to uranium in Table V.[20,95]

Satellites of x-ray lines. Calculations have been made of the energies of x-ray satellites for multiply

TABLE V. Structure of the atomic shell of neutral atoms and the first ground states of their ions for $1 \leqslant Z \leqslant 92$.[95]

Z	Symbol	Structure	Degree of ionization		
			1	2	3
1	H	$1s^1$	—	—	—
2	He	$1s^2$	$1s^1$	—	—
3	Li	$1s^22s^1$	$1s^2$	$1s^1$	—
4	Be	$1s^22s^2$	$1s^22s^1$	$1s^2$	$1s^1$
5	B	$1s^22s^22p^1$	$1s^22s^2$	$1s^22s^1$	$1s^2$
6	C	$1s^22s^22p^2$	$1s^22s^22p^1$	$1s^22s^2$	$1s^22s^1$
7	N	$1s^22s^22p^3$	$1s^22s^22p^2$	$1s^22s^22p^1$	$1s^22s^2$
8	O	$1s^22s^22p^4$	$1s^22s^22p^3$	$1s^22s^22p^2$	$1s^22s^22p^1$
9	F	$1s^22s^22p^5$	$1s^22s^22p^4$	$1s^22s^22p^3$	$1s^22s^22p^2$
10	Ne	$1s^22s^22p^6$	$1s^22s^22p^5$	$1s^22s^22p^4$	$1s^22s^22p^3$
11	Na	[Ne] $3s^1$	[Ne]	$1s^22s^22p^5$	$1s^22s^22p^4$
12	Mg	[Ne] $3s^2$	[Ne] $3s^1$	[Ne]	$1s^22s^22p^5$
13	Al	[Ne] $3s^23p^1$	[Ne] $3s^2$	[Ne] $3s^1$	[Ne]
14	Si	[Ne] $3s^23p^2$	[Ne] $3s^23p^1$	[Ne] $3s^2$	[Ne] $3s^1$
15	P	[Ne] $3s^23p^3$	[Ne] $3s^23p^2$	[Ne] $3s^23p^1$	[Ne] $3s^2$
16	S	[Ne] $3s^23p^4$	[Ne] $3s^23p^3$	[Ne] $3s^23p^2$	[Ne] $3s^23p^1$
17	Cl	[Ne] $3s^23p^5$	[Ne] $3s^23p^4$	[Ne] $3s^23p^3$	[Ne] $3s^23p^2$
18	Ar	[Ne] $3s^23p^6$	[Ne] $3s^23p^5$	[Ne] $3s^23p^4$	[Ne] $3s^23p^3$
19	K	[Ar] $4s^1$	[Ar]	[Ne] $3s^23p^5$	[Ne] $3s^23p^4$
20	Ca	[Ar] $4s^2$	[Ar] $4s^1$	[Ar]	[Ne] $3s^23p^5$
21	Sc	[Ar] $3d^14s^2$	[Ar] $3d^14s^1$	[Ar] $3d^1$	[Ar]
22	Ti	[Ar] $3d^24s^2$	[Ar] $3d^24s^1$	[Ar] $3d^2$	[Ar] $3d^1$
23	V	[Ar] $3d^34s^2$	[Ar] $3d^4$	[Ar] $3d^3$	[Ar] $3d^2$
24	Cr	[Ar] $3d^54s^1$	[Ar] $3d^5$	[Ar] $3d^4$	[Ar] $3d^3$
25	Mn	[Ar] $3d^54s^2$	[Ar] $3d^54s^1$	[Ar] $3d^5$	[Ar] $3d^4$
26	Fe	[Ar] $3d^64s^2$	[Ar] $3d^64s^1$	[Ar] $3d^6$	[Ar] $3d^5$
27	Co	[Ar] $3d^74s^2$	[Ar] $3d^8$	[Ar] $3d^7$	[Ar] $3d^6$
28	Ni	[Ar] $3d^84s^2$	[Ar] $3d^9$	[Ar] $3d^8$	[Ar] $3d^7$
29	Cu	[Ar] $3d^{10}4s^1$	[Ar] $3d^{10}$	[Ar] $2d^9$	[Ar] $3d^8$
30	Zn	[Ar] $3d^{10}4s^2$	[Ar] $3d^{10}4s^1$	[Ar] $3d^{10}$	[Ar] $3d^9$
31	Ca	[Ar] $3d^{10}4s^24p^1$	[Ar] $3d^{10}4s^2$	[Ar] $3d^{10}4s^1$	[Ar] $3d^{10}$
32	Ge	[Ar] $3d^{10}4s^24p^2$	[Ar] $3d^{10}4s^24p^1$	[Ar] $3d^{10}4s^2$	[Ar] $3d^{10}4s^1$
33	As	[Ar] $3d^{10}4s^24p^3$	[Ar] $3d^{10}4s^24p^2$	[Ar] $3d^{10}4s^24p^1$	[Ar] $3d^{10}4s^2$
34	Se	[Ar] $3d^{10}4s^24p^4$	[Ar] $3d^{10}4s^24p^3$	[Ar] $3d^{10}4s^24p^2$	[Ar] $3d^{10}4s^24p^1$
35	Br	[Ar] $3d^{10}4s^24p^5$	[Ar] $3d^{10}4s^24p^4$	[Ar] $3d^{10}4s^24p^3$	[Ar] $3d^{10}4s^24p^2$
36	Kr	[Ar] $3d^{10}4s^24p^6$	[Ar] $3d^{10}4s^24p^5$	[Ar] $3d^{10}4s^24p^4$	[Ar] $3d^{10}4s^24p^3$
37	Rb	[Kr] $5s^1$	[Kr]	[Ar] $3d^{10}4s^24p^5$	[Ar] $3d^{10}4s^24p^4$
38	Sr	[Kr] $5s^2$	[Kr] $5s^1$	[Kr]	[Ar] $3d^{10}4s^24p^5$
39	Y	[Kr] $4d^15s^2$	[Kr] $5s^2$	[Kr] $5s^1$	[Kr]
40	Zr	[Kr] $4d^25s^2$	[Kr] $4d^25s^1$	[Kr] $4d^2$	[Kr] $4d^1$
41	Nb	[Kr] $4d^45s^1$	[Kr] $4d^4$	[Kr] $4d^3$	[Kr] $4d^2$
42	Mo	[Kr] $4d^55s^1$	[Kr] $4d^5$	[Kr] $4d^4$	[Kr] $4d^3$
43	Tc	[Kr] $4d^55s^2$	[Kr] $4d^55s^1$	[Kr] $4d^5$	[Kr] $4d^4$
44	Ru	[Kr] $4d^75s^1$	[Kr] $4d^7$	[Kr] $4d^6$	[Kr] $4d^5$
45	Rh	[Kr] $4d^85s^1$	[Kr] $4d^8$	[Kr] $4d^7$	[Kr] $4d^6$
46	Pa	[Kr] $4d^{10}$	[Kr] $4d^9$	[Kr] $4d^8$	[Kr] $4d^7$
47	Ag	[Kr] $4d^{10}5s^1$	[Kr] $4d^{10}$	[Kr] $4d^9$	[Kr] $4d^8$
48	Cd	[Kr] $4d^{10}5s^2$	[Kr] $4d^{10}5s^1$	[Kr] $4d^{10}$	[Kr] $4d^9$
49	In	[Kr] $4d^{10}5s^25p^1$	[Kr] $4d^{10}5s^2$	[Kr] $4d^{10}5s^1$	[Kr] $4d^{10}$
50	Sn	[Kr] $4d^{10}5s^25p^2$	[Kr] $4d^{10}5s^25p^1$	[Kr] $4d^{10}5s^2$	[Kr] $4d^{10}5s^1$
51	Sb	[Kr] $4d^{10}5s^25p^3$	[Kr] $4d^{10}5s^25p^2$	[Kr] $4d^{10}5s^25p^1$	[Kr] $4d^{10}5s^2$
52	Te	[Kr] $4d^{10}5s^25p^4$	[Kr] $4d^{10}5s^25p^3$	[Kr] $4d^{10}5s^25p^2$	[Kr] $4d^{10}5s^25p^1$
53	I	[Kr] $4d^{10}5s^25p^5$	[Kr] $4d^{10}5s^25p^4$	[Kr] $4d^{10}5s^25p^3$	[Kr] $4d^{10}5s^25p^2$
54	Xe	[Kr] $4d^{10}5s^25p^6$	[Kr] $4d^{10}5s^25p^5$	[Kr] $4d^{10}5s^25p^4$	[Kr] $4d^{10}5s^25p^3$
55	Cs	[Xe] $6s^1$	[Xe]	[Kr] $4d^{10}5s^25p^5$	[Kr] $4d^{10}5s^25p^4$
56	Ba	[Xe] $6s^2$	[Xe] $6s^1$	[Xe]	[Kr] $4d^{10}5s^25p^5$
57	La	[Xe] $5d^16s^2$	[Xe] $5d^2$	[Xe] $5d^1$	[Xe]
58	Ce	[Xe] $4f^26s^2$	[Xe] $4f^15d^2$	[Xe] $4f^2$	[Xe] $4f^1$
59	Pr	[Xe] $4f^36s^2$	[Xe] $4f^36s^1$	[Xe] $4f^3$	[Xe] $4f^2$
60	Nd	[Xe] $4f^46s^2$	[Xe] $4f^46s^1$	[Xe] $4f^4$	[Xe] $4f^3$
61	Pm	[Xe] $4f^56s^2$	[Xe] $4f^56s^1$	[Xe] $4f^5$	[Xe] $4f^4$
62	Sm	[Xe] $4f^66s^2$	[Xe] $4f^66s^1$	[Xe] $4f^6$	[Xe] $4f^5$
63	Eu	[Xe] $4f^76s^2$	[Xe] $4f^76s^1$	[Xe] $4f^7$	[Xe] $4f^6$
64	Gd	[Xe] $4f^75d^16s^2$	[Xe] $4f^75d^16s^1$	[Xe] $4f^75d^1$	[Xe] $4f^7$
65	Tb	[Xe] $4f^96s^2$	[Xe] $4f^96s^1$	[Xe] $4f^9$	[Xe] $4f^8$
66	Dy	[Xe] $4f^{10}6s^2$	[Xe] $4f^{10}6s^1$	[Xe] $4f^{10}$	[Xe] $4f^9$
67	Ho	[Xe] $4f^{11}6s^2$	[Xe] $4f^{11}6s^1$	[Xe] $4f^{11}$	[Xe] $4f^{10}$
68	Er	[Xe] $4f^{12}6s^2$	[Xe] $4f^{12}6s^1$	[Xe] $4f^{12}$	[Xe] $4f^{11}$
69	Tm	[Xe] $4f^{13}6s^2$	[Xe] $4f^{13}6s^1$	[Xe] $4f^{13}$	[Xe] $4f^{12}$
70	Yb	[Xe] $4f^{14}6s^2$	[Xe] $4f^{14}6s^1$	[Xe] $4f^{14}$	[Xe] $4f^{13}$
71	Lu	[Xe] $4f^{14}5d^16s^2$	[Xe] $4f^{14}6s^2$	[Xe] $4f^{14}6s^1$	[Xe] $4f^{14}$
72	Hf	[Xe] $4f^{14}5d^26s^2$	[Xe] $4f^{14}5d^16s^2$	[Xe] $4f^{14}5d^2$	[Xe] $4f^{14}5d^1$
73	Ta	[Xe] $4f^{14}5d^36s^2$	[Xe] $4f^{14}5d^26s^1$	[Xe] $4f^{14}5d^3$	[Xe] $4f^{14}5d^2$
74	W	[Xe] $4f^{14}5d^46s^2$	[Xe] $4f^{14}5d^16s^1$	[Xe] $4f^{14}5d^4$	[Xe] $4f^{14}5d^3$
75	Re	[Xe] $4f^{14}5d^56s^2$	[Xe] $4f^{14}5d^26s^1$	[Xe] $4f^{14}5d^5$	[Xe] $4f^{14}5d^4$
76	Os	[Xe] $4f^{14}5d^66s^2$	[Xe] $4f^{14}5d^36s^1$	[Xe] $4f^{14}5d^6$	[Xe] $4f^{14}5d^5$
77	Ir	[Xe] $4f^{14}5d^76s^2$	[Xe] $4f^{14}5d^76s^1$	[Xe] $4f^{14}5d^7$	[Xe] $4f^{14}5d^6$
78	Pt	[Xe] $4f^{14}5d^96s^1$	[Xe] $4f^{14}5d^9$	[Xe] $4f^{14}5d^8$	[Xe] $4f^{14}5d^7$
79	Au	[Xe] $4f^{14}5d^{10}6s^1$	[Xe] $4f^{14}5d^{10}$	[Xe] $4f^{14}5d^9$	[Xe] $4f^{14}5d^8$
80	Hg	[Xe] $4f^{14}5d^{10}6s^2$	[Xe] $4f^{14}5d^{10}6s^1$	[Xe] $4f^{14}5d^{10}$	[Xe] $4f^{14}5d^9$
81	Tl	[Hg] $6p^1$	[Hg]	[Xe] $4f^{14}5d^{10}6s^1$	[Xe] $4f^{14}5d^{10}$
82	Pb	[Hg] $6p^2$	[Hg] $6p^1$	[Hg]	[Xe] $4f^{14}5d^{10}6s^1$
83	Bi	[Hg] $6p^3$	[Hg] $6p^2$	[Hg] $6p^1$	[Hg]
84	Po	[Hg] $6p^4$	[Hg] $6p^3$	[Hg] $6p^2$	[Hg] $6p^1$
85	At	[Hg] $6p^5$	[Hg] $6p^4$	[Hg] $6p^3$	[Hg] $6p^2$
86	Rn	[Hg] $6p^6$	[Hg] $6p^5$	[Hg] $6p^4$	[Hg] $6p^3$
87	Fr	[Rn] $7s^1$	[Rn]	[Hg] $6p^5$	[Hg] $6p^4$
88	Ra	[Rn] $7s^2$	[Rn] $7s^1$	[Rn]	[Hg] $6p^5$
89	Ac	[Rn] $6d^17s^2$	[Rn] $7s^2$	[Rn] $7s^1$	[Rn]
90	Th	[Rn] $6d^27s^2$	[Rn] $6d^27s^1$	[Rn] $5f^16d^1$	[Rn] $5f^1$
91	Pa	[Rn] $5f^26d^17s^2$	[Rn] $5f^27s^2$	[Rn] $5f^27s^1$	[Rn] $5f^2$
92	U	[Rn] $5f^36d^17s^2$	[Rn] $5f^37s^2$	[Rn] $5f^37s^1$	[Rn] $5f^3$

charged ions formed by the removal of electrons from the outer shells of Ne (Ref. 96), Ar (Ref. 97), Br (Ref. 98), Mo (Ref. 99), Xe (Ref. 100), Pb (Ref. 80), and U (Ref. 101). For Ar, the influence of not only outer vacancies but also mixed states of outer and inner vacancies is considered. For Ne, Ar, Br, Mo, and Xe, the energies of the x-ray satellites are calculated for the ground state of the ion; for Pb and U only the ionization states that arise on the removal of the electrons with the highest quantum numbers are considered.

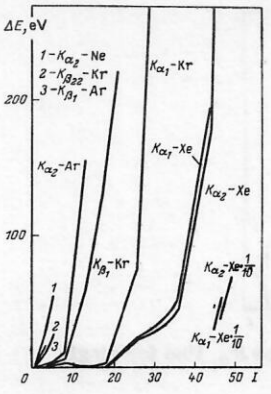

FIG. 2. Energy shifts of characteristic x-ray transitions of noble gases up to Xe as functions of the number I of outer vacancies.

The energy shifts of the characteristic x-ray radiation of some transitions of the K, L, and M series of the noble gases shown in Figs. 2 and 3 were obtained by the Dirac–Fock–Slater method using the Slater exchange potential ($C = m = n = 1$) and Latter's correction[72] for the Coulomb potential at large distances from the nucleus. For the transitions of all series a rule can be formulated: The energy shifts are greatest for the x-ray series whose initial level has the largest principal quantum number. The change in the satellite energy for some x-ray transitions with increasing degree of ionization is not monotonic. For example, for transitions of the K and L series of elements with closed $4f$ subshells, shifts of the x-ray transitions to lower energies are observed. The lines of the M series do not have this property. This fact can be used for diagnosis of ionization states to eliminate the ambiguity in the interpretation of the x-ray spectra of the K and L series. The extent to which the outer vacancies influence the x-ray transition energies depends strongly on the electron levels that participate in the considered transition.

Generally speaking, the change in the energy shifts of the x-ray K transitions is greatest in the cases when the

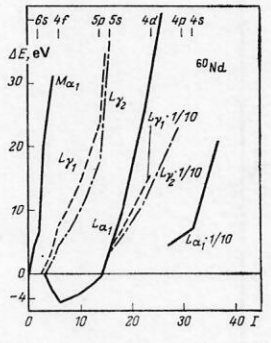

FIG. 3. Energy shifts of transitions of the L and M series of Nd as functions of the number I of external vacancies. The completely stripped shells are indicated at the top.

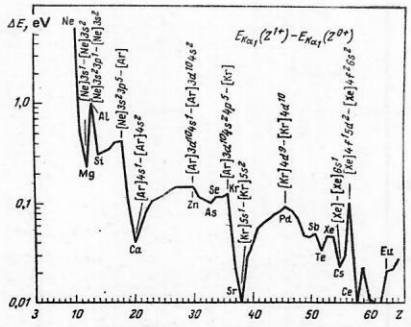

FIG. 4. Dependence of the shift of the K_{α_1} line for singly ionized ions on Z.[99]

difference between the principal quantum numbers of the electron states is maximal. This rule is also valid for the other series. The reason for this is the different decreases in the binding energies of electrons in the states that participate in the x-ray transition on the appearance of an additional outer vacancy. There is a general characteristic tendency: With increasing principal quantum number of the vacancies in the outer shells their influence decreases. The growth of the binding energy of the outer electron states is also diminished. The relative change in the binding energy increases with increasing difference between the principal quantum numbers of the considered levels. This effect will be discussed in more detail below.

The energy shifts of the K_{α_1} and L_{α_1} transitions for singly ionized atoms with $Z \leq 70$ are given in Figs. 4 and 5. In all cases there are characteristic local maxima of the shifts of the x-ray energies for the noble gases. The energy shift decreases for the elements following each noble gas, and reaches a minimum in Mg, Ca, Sr, and Ce for the K_{α_1} transitions and in Tc and Ce for the L_{α_1} transition. As a rule, these minima are associated with transitions in atoms and singly ionized ions that have the shell structure of noble gases with additional ns electrons ($n = 3, 4, 5, 6$). The ionization of the ns electrons leads to a relatively small shift in the binding energy of the electron states participating

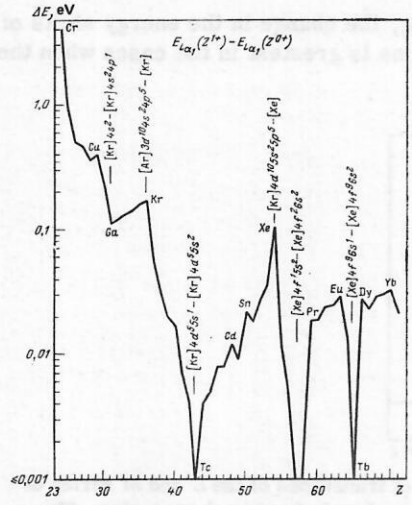

FIG. 5. Dependence of the shift of the L_{α_1} line for singly ionized ions on Z.[99]

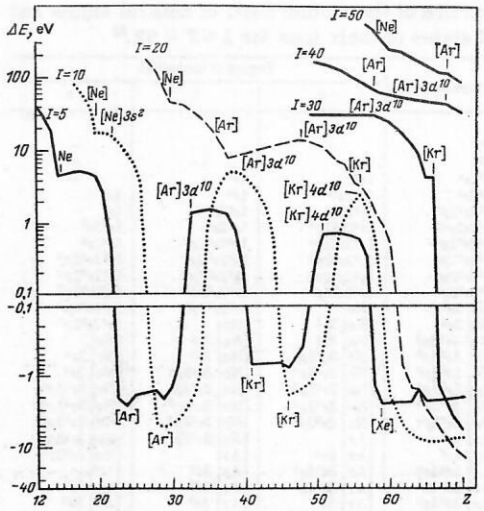

FIG. 6. Dependence of the shift of the K_{α_1} line for I-fold ionized ions on Z.[99]

in the transition. The removal of electrons with large angular momenta gives large shifts of the x-ray energies because the difference between the electron binding energies then changes more strongly. An exception to the rule is the minimum at $Z = 58$. Here we observe a deviation in the filling of the electron shells of the ground state of the neutral atom ($[Xe]4f^2 5d^0 6s^2$) and the ground state of the singly ionized ion ($[Xe]4f^1 5d^2$). The following regularity consists of a decrease in the energy shifts of the x-ray transitions with increasing atomic number of the noble gases due to the weak change in the intra-atomic screening of the electrons.

A fuller picture of the x-ray transition energy shifts of multiply charged ions for elements with $Z \leq 70$ is given by Figs. 6 and 7. At degrees of ionization corresponding to closed subshells, we observe characteristic changes in the gradient of the energy shifts. At degree of ionization 5, the K_{α_1} line and, with some exceptions, the L_{α_1} line have local minima of the shifts for the

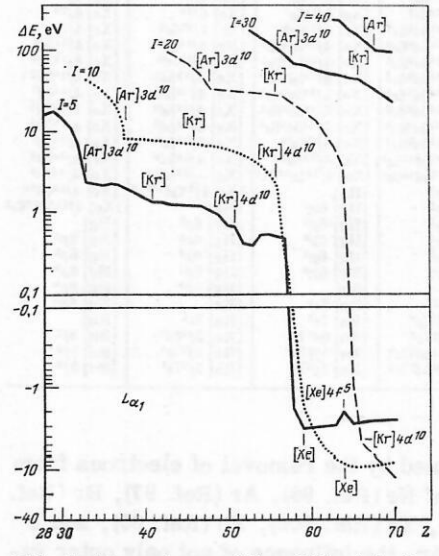

FIG. 7. Dependence of the shift of the L_{α_1} line for I-fold ionized ions on Z.[99]

atomic configurations corresponding to those of the noble gases. As the s and p levels are filled, the energy shifts for K_{α_1} transitions decrease, while they increase as the d levels are filled. For L_{α_1} transitions at fixed degree of ionization, the shifts decrease with increasing Z.

Useful information for identification of the charge state of an ion on the basis of the energy of its characteristic x-ray radiation is contained in Figs. 4–7. For a large Z range there are no intersections of the shifts for different degrees of ionization of atoms with definite Z, i.e., the measured shifts correspond to a definite degree of ionization of the atom. If the shifts do intersect, the situation becomes ambiguous, i.e., for the correct determination of the charge state of the atom additional, independent information is required.

Chemical energy shifts of x-ray transitions. Systematic investigations of the chemical shifts make it possible to obtain information about the valence structure of the electrons in different regions of the periodic table. The existence of chemical shifts was first established by Lindh and Lundquist,[102] who determined the relative intensities and wavelengths of lines of the K_β group of some compounds of S with metals and with S itself.

Fundamental studies to determine the chemical shifts were made by the Leningrad group of Sumbaev. In 1965, this group reported the first measurements of the chemical shifts of the K_{α_1} energy of molybdenum and tin.[103] This group also investigated various compounds of silver, antimony, tungsten, and rare-earth elements. At the same time, the results were published of measurements for tin,[104] ruthenium, praseodymium, and ytterbium.[105]

The influence of the chemical valence states on the x-ray emission spectra is determined by the valence electrons. Removal of a valence electron from an atom leads (this is especially true for s electrons) to a decrease in the screening of the nuclear potential for the other electrons, and the binding energy of these electrons increases (Fig. 8). In atoms with medium values of Z, the change in the electron binding energies reaches 10 eV and, as a rule, is approximately the same for the $1s$, $2p$, $3p$, and $4p$ electron levels, with which the most intense x-ray transitions of the K series are associated. As a consequence, the change in the energy of the x-ray K transitions is two orders of magnitude smaller, i.e., the chemical energy shift of the x-ray K transitions is about 0.1 eV. This effect is particularly clearly manifested in inner shells. Therefore, most investigations of the chemical energy shifts

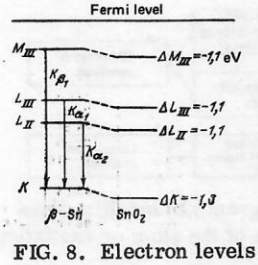

FIG. 8. Electron levels in Sn and SnO_2.[106]

TABLE VI. Experimental values of the chemical shifts of x-ray transitions of the K series (all shifts are given in meV; $\Delta E = E_B - E_A$).

Investigated pairs A	Investigated pairs B	$\Delta E_{K_{\alpha_1}}$	$\Delta E_{K_{\alpha_2}}$	$\Delta E_{K_{\beta_1}}$	$\Delta E_{K_{\beta_2}}$	$\Delta E_{K_{\beta_{1,2}}}$	References
Rb	RbCl	21±4	–	28±10	131±22	–	[109]
Zr	ZrO_2	−299±5	–	−149±8	480±15	–	[109]
Mo	MoO_3	−199±5	–	−137±15	224±15	–	[108, 109]
Ru	RuO_2	−42±4	–	–	−24±25	–	[105]
	RuF_3	−94±3	–	–	−50±25	–	[105]
Ag	Ag_2S	54±4	–	59±10	−125±15	–	[108, 109]
	AgCl	122±5	–	129±9	−104±16	–	[108, 109]
Snα	SnO_2	210±10	–	193±16	101±36	–	[104, 109]
Snβ	SnO	–	–	122±11	89±21	–	[109]
PrF_3	Pr	−45±4	–	–	48±29	–	[105]
	PrC_2	5±10	5±10	–	–	–	[105]
	PrO_3	−94±6	−48±6	–	−31±9	−11±10	[105]
	$PrFeO_3$	–	–	–	−127±35	−309±7	[105]
	Pr_6O_{11}	−214±8	−214±8	–	–	–	[105]
	PrO_2	−320±5	−320±5	–	−416±18	−1018±4	[105]
$SmCl_2$	SmF_3	−606±14	−488±19	–	−415±50	β_1: −1455±40	[109]
						β_3: −1360±50	[109]
EuF_2	EuF_3	−644±11	−582±19	–	−300±65	β_1: −1450±46	[109]
						β_3: −1730±50	[109]
Yb	YbF_3	−579±26	−570±14	–	−586±114	−1402±43	[105]
	Yb_2O_3	−592±26	−564±14	–	−839±119	−1676±62	[105]

of x-ray transitions are based on analysis of the K-series spectra. It is characteristic that the absolute shift in the binding energy has the largest values for electrons of the K shells and decreases for the outer levels. The largest effect is observed for the most intense components of the x-ray series. It should be noted that the removal of an electron from an atom in a chemical compound need not necessarily be complete; the energy shift is related to the ionicity of the compound. The chemical shifts are largest for light elements whose valence electrons are localized in the L shell and have a large influence on the binding energies of the electrons of the K shell. Experimental results for the chemical shifts of the K transitions are given in Table VI.[106,107]

Certain regularities can be seen in the data of Table VI. Thus, the chemical shifts increase with increasing Z from Ag to Sn as the valence $5s$ and $5p$ shells are filled with electrons. The largest chemical shifts are observed for the rare-earth elements. These shifts are explained by the large changes in the screening of the inner electrons that arise when electrons of the $4f$ subshells are added or removed. The changes in the energies of the x-ray transitions between different levels (see Table VI) indicate different sensitivities of the electron levels to the chemical valence states, this being revealed by the different values of the chemical shifts.

The development of the self-consistent field method and the accessibility of sufficiently large computers made possible quantitative comparisons of the experimental values and calculated results[105,109,110] and thus the verification of structural ideas about the nature of the chemical bond.

Influence of Inner Vacancies on the Energies of x-Ray Transitions. *Theoretical investigations.* Weak lines in the short-wavelength region of the most intense diagram lines for the x-ray K, L, and M series were long known. Initially, these were called *nondiagram* lines because their energy cannot be obtained from the energy-level diagrams of the emitting atom in the presence

of one inner vacancy. Because of their low intensity and appearance in the energy neighborhood of the diagram lines, they were called *satellite* lines.

Satellite lines were observed for the first time by Siegbahn and Stenström[111] in 1916 in the x-ray emission K spectra of the elements with $11 \leq Z \leq 30$. Satellite lines of the L series were first observed by Coster[112] in 1922 for the $37 \leq Z \leq 51$ elements. These satellites were investigated in more detail by Richtmyer.[113] The first satellite lines of the M series were discovered in 1918 in experiments of Stenström,[114] which were immediately continued by other authors.[115,116]

The first explanation of the origin of the satellite lines was given by Wentzel[117,118] in 1921. According to his theory, the difference between the frequencies of the individual K_α satellite lines is associated with single-electron transitions in atoms with several inner vacancies. For each K_α satellite, Wentzel proposed special electron transitions, which proved to be a mistake. A following modification of Wentzel's theory was made to interpret the separation of the frequencies of K_{β_1}, L_{β_2}, L_{γ_1}, and $L_{\gamma_{2\ 3}}$ satellites.[119] Ray[120] was the first to take into account the multiplet nature of the energy levels. On this basis, he succeeded in predicting multiplets consisting of six satellites of K_α transitions, for which he gave the spectroscopic designations. Investigations into the origin of the satellites were continued by Kennard and Ramberg[121] on the basis of Hartree's method. Good agreement between the calculated and experimental values of the frequency shifts is achieved if one assumes that KL ionization is the reason for the occurrence of the K'_α, K_{α_3}, and K_{α_4} satellites and that KL^2 ionization is responsible for the $K_{\alpha_{5,6}}$ and $K_{\alpha_{7,8}}$ satellites. The long-time open question of the exact description of the satellites of the L and M series was solved by the theory of Coster and Kronig,[122] which solved the problem of the mechanism of occurrence of states with several vacancies in the inner shells of an atom. The theory is based on the importance of Auger transitions for the formation of secondary vacancies in inner shells. The primary vacancy arises as a result of electron impact or photoionization. The Coster–Kronig theory revolutionized ideas about the occurrence of x-ray satellites and was able to explain all aspects of the L satellites. In addition, on the basis of the theory the origin of the M_{α_1} and M_β satellites was clarified,[123] namely the M_{α_1} satellites are associated with ionization of the M_V, $N_{VI,VII}$ levels, and the M_β satellites with the ionization of the M_{IV}, $N_{VI,VII}$ levels. The energies of all known satellite lines resulting from electron impact or photoionization are given in the tables of wavelengths in Ref. 124.

Satellites in the case of multiple ionization by electron impact and photoionization. Ionization by electron impact and photoionization are characterized by the excitation of diagram lines formed by the appearance of isolated primary vacancies. Only slight multiple KL^1 and KL^2 ionization is observed (Fig. 9). Besides the short-wave satellites of the diagram lines, long-wave satellites are observed. A number of long-wave satellites are explained by electron transitions from outer

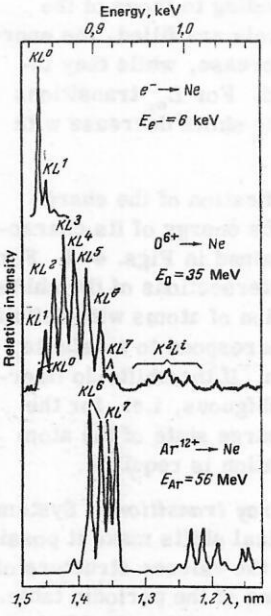

FIG. 9. Spectra of K x rays of Ne produced by collisions with electrons and heavy ions.[125]

levels of the atom to the K level of a different ion in a crystal (cross transitions) and two-electron processes with a decrease in the x-ray transition energy due to the simultaneous excitation of an outer electron (radiative Auger transition).[126–128] Data on the transitions and structures that arise in the case of electron or fluorescence excitation are given in Fig. 10.[126] The figure does not take into account the structures that arise in the case of ion–atom collisions. Figure 10 is discussed in detail in Ref. 129.

Application of the frozen-orbital approximation to atoms with closed and partly closed shells, molecules, and solids makes it possible to interpret the diagram lines and the structures that arise as a result of multiplet splitting and cross transitions. Only single-electron transitions between singly ionized configurations are considered. If one gives up the frozen-orbital approximation and takes into account the processes of rearrangement of the atomic shell that follow after direct and indirect multiple ionization, the appearance of short-wave satellites can be explained. The long-wave satellites can be explained by many-electron processes.

If there is sufficiently strong interaction between an unfilled subshell and an x-ray vacancy, the multiplet

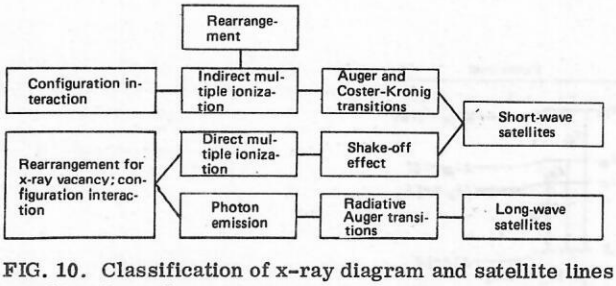

FIG. 10. Classification of x-ray diagram and satellite lines resulting from fluorescent excitation of the atom or excitation by electron impact.[129]

structure of x-ray emission lines may be manifested in the form of splitting, so that the long-wave satellites of a line emitted by atoms with unfilled d or f subshells can be ascribed to multiplet splitting.[130]

A number of weak satellites of the principal maxima of the emission bands of molecules and solids can be explained by the proximity of the valence orbitals of the emitting atom to orbitals of surrounding atoms. These satellites, which were observed for the first time in the K spectra of KCl and NaCl,[131] can be explained by transitions of valence electrons of an ion in the crystal to a K vacancy of a different ion.

If in the case of an x-ray transition that corresponds to a diagram line a further electron is missing in some shell, then the energy of the emitted photon exceeds the energy of the diagram line, i.e., a weak short-wave satellite of the diagram line occurs with small probability.

Of all the conceivable ways in which multiply ionized atoms could be formed (successive ionization by several electrons, multiple ionization as a result of nonradiative transitions, multiple ionization by electron impact and multiple photoionization), indirect multiple ionization and direct multiple ionization (shake-off process) are the most probable because of the short lifetime of an electron vacancy (a K vacancy for $Z = 40$ has a lifetime of about 2×10^{-16} sec; for $Z = 90$, about 8×10^{-18} sec). Particularly important are processes of the type $X_i - X_jY$, in which the valence states X_i and X_j correspond to different subshells of one principal shell. Such processes are known in the literature as Coster–Kronig transitions.

The fundamentals of the theory of the shake-off effect and corresponding numerical results can be found in Refs. 132–135. The essence of this theory is that when one electron is removed a second electron goes over to an excited bound state or to the continuum. The excitation occurs as a result of a "sudden" change in the atomic potential, which happens if an electron is removed during a time short compared with the orbital period of the second electron.

The probability of shake-off of a second electron has the largest values for weakly bound electrons. For a given shell, the ionization probability decreases as Z_{eff}^{-2} (Z_{eff} is the effective charge of the nucleus). The dependence of the probability of the shake-off effect on Z is shown in Fig. 11. The change in the charge of the ion on ionization of the K shell corresponds approximately to transition to a nucleus with charge $Z + 1$. In the frozen-orbital approximation, the shake-off probability does not depend on the method or energy of the excitation. This is valid until the excitation energy exceeds the ionization potential. A detailed model representation of the shake-off effect is given in Ref. 132. As a rule, the energy of the emitted electrons produced by the effect is small. Most of the electrons have kinetic energy lower than the corresponding binding energy.[137–139] For estimates of the intensity of the shake-off processes we can formulate the following rules[136]:

1) for a given subshell, the shake-off effects decrease

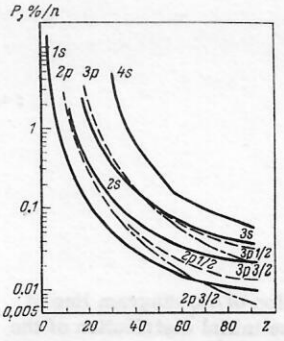

FIG. 11. Probability of the shake-off effect for P electrons for different subshells in nuclear β^- decay as a function of the atomic number Z. The probabilities are divided by the number of electrons in the subshell.[133]

with increasing Z;

2) for a given atom and fixed angular momentum, the intensity increases with increasing principal quantum number;

3) for a given principal quantum number, the shake-off probability is higher for large angular momenta at low Z; at high Z, the opposite tendancy is observed;

4) the total contribution of the shake-off effect to the ionization cross section of an atom, summed over all subshells, is almost independent of Z.

A review of studies of direct multiple ionization is given in Refs. 132 and 140. Emission of x rays by multiply ionized atoms is almost always associated with a satellite short-wave structure of the diagram lines, the satellites either coinciding with the diagram lines or lying in the short-wave region of them (in the presence of vacancies in the outer shells). The different forms of satellite lines that arise as a result of transitions between multiply ionized states of the types LM, LN, LMM, and LNN are given in Fig. 12. It follows from calculations of the corresponding transition energies that because of the appreciable widths of the satellite lines (the natural width of the x-ray lines) only some of of these lines can be observed experimentally, i.e., they can be separated in the x-ray spectrum. The satellites with initial vacancies in LM, LMM, or LMN states are separated from the diagram line by a few electron volts and appear on the short-wave side. Satellites with initial vacancies in the LN or LNN states coincide with the diagram lines. For the zirconi-

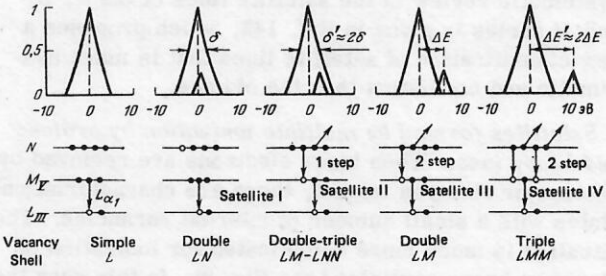

FIG. 12. Schematic illustration of the formation of satellites and their energy position in the spectrum of the L series of Zr ($Z = 40$).[140]

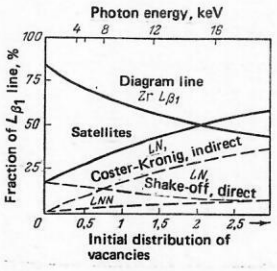

FIG. 13. Dependence of composition of L_{β_1} diagram line of Zr on the excitation energy and the initial distribution of the vacancy-number ratio $L_I/(L_{II}+L_{III})$.[141]

um L_{β_1} diagram line, Fig. 13 shows the proportions of the satellites resulting from the decay of an $L_{II}N$ vacancy formed by direct and indirect multiple ionization and of triply ionized $L_{II}NN$ states formed by an Auger transition in a doubly ionized atom in the LM state or by a combination of direct and indirect multiple ionization in the N shell. With increasing energy of the exciting photons, the ionization cross section of the $2s$ shell of zirconium decreases more slowly than the corresponding cross section of the $2p$ shell, and therefore the vacancy ratio $L_I/(L_{II}+L_{III})$ increases. With increasing probability of Coster–Kronig transitions, the contribution of the diagram lines decreases. Even at very low excitation energies, there can be appreciable superposition of satellites on a diagram line, provided the employed excitation energy is not higher than the excitation energy of the singly ionized state by only a few electron volts.

Besides electron or photon excitation, radiative Auger transitions can give rise to satellite lines. The energy of the emitted γ rays is

$$h\nu = E_i - E_{ff'} - E_e.$$

The difference between the energies E_i of the singly ionized state and $E_{ff'}$ of the doubly ionized final state corresponds to the energy of the nonradiative Auger transition $i \to ff'$. The energies of the emitted or excited electrons have discrete negative values corresponding to bound states below the energy zero point and a continuous spectrum in the direction of positive values. The maximal kinetic energy of an electron is $E_e = E_i - E_{ff'}$. Accordingly, the radiation is characterized by a steep drop in the short-wave part of the spectrum and a slow fall in the long-wave part. The theory of radiative Auger transitions is given in Ref. 135. A systematic review of the satellite lines of the K, L, and M series is given in Ref. 142, which proposes a new classification of satellite lines that is more systematic and consistent than the old one.

Satellites formed by multiple ionization by protons and heavy ions. When inner electrons are removed by photons or electron impact, there are characteristically states with a small number of internal vacancies. The situation is much more complicated for ionization of atoms by heavy particles (see Fig. 9). In this case there are configurations with a set of vacancies. It is not uncommon to encounter one-, two-, and three-electron systems. High-resolution x-ray spectroscopy and Auger-electron spectroscopy have been used to investigate a large number of characteristic spectra resulting from ion–atom collisions. Analysis of these spectra on the basis of model representations and calculations by the self-consistent field method permits conclusions to be drawn about the interaction mechanism of the collision. The lines of satellites and hypersatellites are identified by means of the calculated energies or wavelengths, respectively. Thus, conclusions are obtained about the distribution of vacancies in atomic shells after ion–atom collisions.

The first experiments in which ionization of inner electron shells was observed after ion–atom collisions were made in 1912–1914.[143–146] In these experiments, various targets were irradiated with α particles from radioactive sources, and the x-ray radiation was observed. The physical picture remained incomplete until Meitner[147] in 1922, Robinson[148] in 1923, and Auger[149,150] in 1925 and 1926 showed that the ionization is accompanied by x-ray emission and additional electron emission. The existence of two independent ways in which the atomic shell can be rearranged restricts the possibilities of exact experimental determination of the ionization cross section. If a vacancy appears in a definite subshell as a result of a collision, the transition cross section is characterized by the cross sections for the production of x-ray photons and Auger electrons only for K ionization. Measurement of the ionization cross sections for the $L, M, \ldots$ subshells is complicated by a third effect, discovered in 1935 by Coster and Kronig,[122] in which there is a rearrangement of the subshells. In multiply ionized atoms the initial distribution of the vacancies is particularly important. The main processes in the case of ionization of atoms by heavy ions will be considered in Sec. 5.

High-resolution x-ray spectroscopy made it possible to obtain much experimental information about KL vacancies for elements up to $Z = 32$. Relatively few systematic studies have been made on XY vacancies in inner shells, in which vacancies are localized in shells different from the K or L shells. The energy shifts of the K_α satellites relative to their diagram lines are shown as functions of the atomic number Z of the incident particle in Fig. 14. As can be seen from the figure, the satellite structure increases with increasing Z. If ionization of one of the inner subshells occurs in

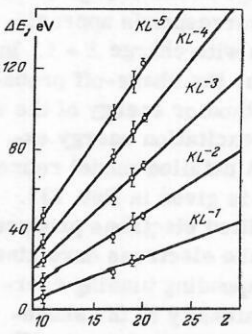

FIG. 14. Dependence of the energy shift ΔE of K_α satellites of light elements in the presence of additional L vacancies[89,94] on the atomic number Z.

TABLE VII. Energy shifts of satellite lines with additional vacancy in the L and M orbitals[152] calculated in accordance with the results of Ref. 151 (Z_L and Z_M are the estimated screened charges; $Z_L = Z - 4.15$; $Z_{M_{I,II,III}} = Z - 11.25$; $Z_{M_{IV,I}} = Z - 21.15$).

Transition	Initial vacancy	Final vacancy	Shift for L vacancy, eV	Shift for M vacancy, eV
K_α	K	$L_{II,\ III}$	$1.66Z_L$	$0.06Z_M$
$K_{\beta 3,1}$	K	$M_{II,\ III}$	$4.38Z_L$	$0.91Z_M$
L_α	L_{III}	$M_{IV,\ V}$	$2.24Z_L$	$0.56Z_M$
$L_{\beta 1}$	L_{II}	M_{IV}	$2.24Z_L$	$0.56Z_M$
$L_{\beta 2}$	L_{III}	N_V	$3.71Z_L$	$1.72Z_M$

an ion–atom collision, there is also a high probability of ionization of other subshells due to the strong Coulomb interaction. These additional vacancies frequently exist until the filling of the vacancy in the inner shell. The energy shifts of the satellite lines can be estimated in a calculation from the change in the electron binding energies of the corresponding levels in the presence of simultaneous vacancies in the shells that are situated higher. Using Burch's simple procedure[151] and hydrogenlike wave functions, it is possible to obtain the changes in the binding energies for the K, L, M, and N levels due to simultaneous vacancies in the $2p$ (L) or $3d$ (M) shells. The binding energy increases because of the decrease in the screening of the electrons, and the most strongly bound electrons undergo the largest increase in the binding energy. The energy of the satellites also increases with increasing number of vacancies. In Table VII, we give examples of the strongest transitions of the K and L series. The energy shifts in Table VII are proportional to the screened charge for the L and M electrons found by Slater's method.[153] The results obtained in this way give a good estimate of the expected shifts but are not very accurate for high shells. For a more accurate estimate, one must make self-consistent field calculations. In addition to this consideration of ordinary satellite lines, we should point out that the chemical environment of an atom in a solid influences the satellite structure.[154] The radiative Auger effect and the radiative effects of rearrangement of the electrons give rise to satellites whose energies lie in the long-wave region of the diagram lines.[155,156] Double K transitions, in which two electrons simultaneously fill two K vacancies, correspond to peaks in the satellite spectrum with twice the K_α energy.[157]

Intensities of Radiative Transitions in Multiply Ionized Atoms

Calculation of Intensities of x-Ray Transitions. Additional vacancies in the electron shell influence the probabilities of radiative electron transitions. The intensities of the x-ray and Auger transitions and, thus, the fluorescence yield are changed. The changes in the intensities of the x-ray transitions represent an independent atomic parameter whose measurement yields information about the ionization state of the atom.

Calculations of radiative transitions of inner-shell electrons are part of the more general problem of calculating radiative transitions.[36,158-161] The main problem in atomic-structure calculations is the description of the interaction between the electrons. For inner-shell electrons, the interelectron interaction is relatively weak compared with the interaction between the electrons and the nucleus. Rough approximations here frequently give satisfactory results.

For transitions in atoms of heavy elements, it is important to take into account relativistic effects and the finite wavelength of the x-ray radiation. For transitions between different shells, these two factors are on an equal footing. The corrections to the oscillator strengths due to these effects are greater than 5% for K transitions when $Z > 50$ and for L transitions when $Z > 80$.[31]

In the region of large Z, the importance of multipole transitions increases. In the photoelectric effect, high multipoles are important at high energies; in the x-ray emission spectra only the electric and magnetic dipole and quadrupole radiation has practical importance.

To analyze transitions in multiply ionized atoms, Larkins[162] proposed a statistical procedure of averaging that makes it possible to estimate the fluorescence yield and the oscillator strengths. If there are n electrons in a subshell that can contain n_0 electrons in the closed state, the transition intensity is reduced by n/n_0 times for single-electron transitions and by $n(n-1)/n_0(n_0-1)$ times if two electrons of the partly filled shell participate in a transition. The oscillator strength decreases in proportion to n/n_0. The probability of radiative transitions is proportional to the product of the oscillator strength and the transition energy. For known differences between the binding energies of the electrons that participate in a considered transition, one can take into account the influence of the change in the binding energy on the transition probability. A study of radiative transitions in terms of multipoles was made in Refs. 159 and 163. Relativistic calculations of radiative transitions have been made by Scofield.[31,164,165]

We now discuss the calculation of the relativistic matrix elements for finding the probabilities of radiative transitions in a multipole expansion, following Ref. 31.

In the first order of perturbation theory the intensity of photons emitted with energy $\hbar\omega$ and momentum $\hbar k$ in the angle $d\Omega$ with polarization vector ε by an atom that goes over from state 1 to state 2 is

$$\Gamma_{12} = |\alpha\omega/2\pi| < \Psi_1 | \sum_j \boldsymbol{\alpha}_j \boldsymbol{\varepsilon} \exp(i\mathbf{kr}) | \Psi_2 >|^2 d\Omega.$$

The photon energy is determined by the initial and final energies of the atomic states:

$$\hbar\omega = \hbar kc = E_1 - E_2.$$

To calculate the atomic matrix elements, it is convenient to introduce photon states with definite parity and angular momentum relative to the nucleus. For this, we define a set of vector fields on the unit sphere:

$$Y^{(0)}_{LM}(\hat{r}) = \hat{\mathbf{r}} Y_{LM}(\hat{r});\ Y^{(e)}_{LM}(\hat{r}) = [L(L+1)]^{-1/2}\ \nabla Y_{LM}(\hat{r});$$
$$Y^{(m)}_{LM}(\hat{r}) = [L(L+1)]^{-1/2}\ \mathbf{L} Y_{LM}(\hat{r}),$$

where $\mathbf{L} = -i\mathbf{r} \times \nabla$ and $\mathbf{r}$ is a vector on the unit sphere.

These vector fields are mutually orthogonal, the component with index 0 is perpendicular to the sphere, and the components e and m are tangential.

Plane waves of the radiation field can be decomposed with respect to these vector spherical harmonics:

$$\varepsilon \exp(i\mathbf{kr}) = 4\pi \sum_{L,M} [\varepsilon Y^{(m)*}_{LM}(\hat{k})\, A^{(m)}_{LM}(k, \mathbf{r}) - \varepsilon Y^{(e)*}_{LM}(\hat{k})\, A^{(e)}_{LM}(k, \mathbf{r})];$$

$$A^{(m)}_{LM}(k, \mathbf{r}) = i^L [L(L+1)]^{-1/2} j_L(kr)\, \mathbf{L} Y_{LM}(\hat{r});$$

$$A^{(e)}_{LM}(k, \mathbf{r}) = i^L [L(L+1)]^{-1/2} k^{-1} \nabla \times \mathbf{L} j_L(kr)\, Y_{LM}(\hat{r});$$

here, $j_L(kr)$ are spherical Bessel functions; A is a solenoidal solution of the vector Helmholtz equation $[\nabla^2 + k^2]A = 0$ with angular momentum L and parity $\pi_{em} = (-1)^L$ for waves of electric type and $\pi_{em} = (-1)^{L+1}$ for waves of magnetic type. Using Dirac matrices, we can represent the wave functions of the single-electron states with definite angular momentum as

$$\Phi^{\mu}_{k}(\mathbf{r}) = \frac{1}{r}\begin{pmatrix} G(r)\,\chi^{\mu}_{k} \\ iF(r)\,\chi^{\mu}_{-k} \end{pmatrix}, \tag{15}$$

where

$$\chi^{\mu}_{k}(\hat{r}) = \sum_{m} C\left(l, \tfrac{1}{2}, \mu - m, m; j, \mu\right) Y_{l, \mu-m}(\hat{r})\, \chi^{m}_{1/2};$$

$\chi^{m}_{1/2}$ describes a spinor with spin $\frac{1}{2}$. The quantum numbers j and l are expressed as $j = |k| - \frac{1}{2}$ and $l = |k + \frac{1}{2}| - \frac{1}{2}$. The matrix elements of transitions between the single-particle states have the form

$$\left.\begin{aligned} &\langle j_1 m_1 | \alpha A^{(e)}_{LM} | j_2 m_2 \rangle = -i^L (4\pi)^{-1/2} (2j_2+1)^{1/2} \\ &\times b(k_1, k_2, L)\, R_L(e)\, C(j_2 L m_2 M;\ j_1 m_1); \\ &\langle j_1 m_1 | \alpha A^{(m)}_{LM} | j_2 m_2 \rangle = -i^{L+1} (4\pi)^{-1/2} (2j_2+1)^{1/2} \\ &\times b(k_1, k_2, L)\, R_L(m)\, C(j_2 L m_2 M;\ j_1 m_1). \end{aligned}\right\} \tag{16}$$

The quantities $b(k_1, k_2, L)$ have the form

$$b(k_1, k_2, L) = (-1)^{j_2+L+1/2} [(2l_1+1)(2l_2+1)(2L+1)/L(L+1)]^{1/2} \times \begin{Bmatrix} L & l_2 & l_1 \\ 1/2 & j_1 & j_2 \end{Bmatrix} \begin{pmatrix} L & l_2 & l_1 \\ 0 & 0 & 0 \end{pmatrix}; \tag{17}$$

C are Clebsch–Gordan coefficients; the brackets in (17) characterize the corresponding Racah coefficients and Wigner's $3j$ symbols.

In a spherically symmetric potential, the intensity of transitions between single-particle electron states can be expressed in terms of radial wave functions.[166] The radial matrix elements are

$$R_L(m) = (k_1 + k_2) \int dr\, j_L(kr)\, (F_1 G_2 + G_1 F_2);$$

$$R_L(e) = \int \frac{dr}{kr} \Big[(F_1 G_2 - G_1 F_2)\, L(L+1)\, j_L(kr) + (k_2 - k_1)(F_1 G_2 + G_1 F_2) \left(r \frac{d}{dr} + 1\right) j_L(kr) \Big].$$

The matrix elements are nonvanishing if the conditions $|j_1 - j_2| \leq L \leq j_1 + j_2$ are satisfied; the sum $l_1 + l_2 + L$ must be even and odd, respectively, for electric and magnetic multipoles. If there are n_1 electrons in the initial subshell and $2j_2 + 1 - n_2$ vacancies in the final subshell, the radiation intensity, averaged over the magnetic moments of the final state, has the form (see Refs. 31, 164, and 167–170)

$$\Gamma_{12} = 2\alpha\omega^2 [(2j_2 + 1 - n_2)\, n_1/(2j_1 + 1)] \sum_{L} [f_L(m) + f_L(e)],$$

where

$$f_L(e) = \omega^{-1} (2j_1 + 1)\, b^2(k_1, k_2, L)\, R^2_L(e);$$

$$f_L(m) = \omega^{-1} (2j_1 + 1)\, b^2(-k_1, k_2, L)\, R^2_L(m).$$

To take into account electron exchange effects, it is necessary to make relativistic self-consistent field calculations and obtain wave functions describing the exact initial and final states of the electrons. Neglect of exchange effects in the calculation of the K_β/K_α intensity ratio gives, for example, an error of order 5%.[165] However, if one is merely interested in the relative changes in the x-ray intensities, electron exchange effects can be ignored. In some cases, correlation effects make an important contribution to the oscillator strengths. The applications of perturbation-theory methods to many-body systems for calculations of the probabilities of radiative transitions are reviewed in Ref. 171.

Intensities of x-Ray Transitions in Multiply Ionized Atoms. The development of computers and programs for numerical calculations of atomic structure have made it possible to take into account the electron interaction and, thus, to obtain rather accurate calculated results. The relativistic and nonrelativistic versions of the Hartree–Fock method with the Slater exchange potential are widely used (see Refs. 164, 165, and 172–189). Calculations of the fluorescence yields of highly ionized atoms are made in Refs. 185 and 186. For highly ionized atomic states only a few results are so far known.

The total probability of x-ray K transitions and the K_β/K_α intensity ratio are shown as functions of the outer-shell ionization of Pb in Fig. 15.[80] Following Scofield,[31,164] the calculation was made using relativistic wave functions calculated by the Dirac–Fock method. Allowance was made for all multipoles of the radiation, for retardation effects, and for the influence of the finite size of the nucleus. Electron exchange was not taken into account in the calculation of the wave functions of the initial and the final state, since the main attention was directed toward the change of the considered parameters with increasing degree of ionization. Figure 15 shows clearly the effects of rearrangement of the atom after ionization. These effects are observed in contrast to the results obtained using Larkins's procedure.[162] The results are typical of ionization of electrons from d and f shells. These electrons are unimportant for the radiative de-excitation of K vacancies, but they strongly screen the p electrons, which determine the emission of the K photons. The changes in the total probability of emission for K transitions and the

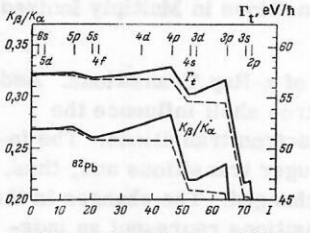

FIG. 15. Dependence of the total probability Γ_t of x-ray K transitions and ratio of the probabilities of x-ray K_β and K_α transitions on the ionization of the outer shells of Pb.[80] The broken lines are the results of using Larkins's procedure[162]; the degree of ionization at which an electron is removed from the indicated shell is shown at the top.

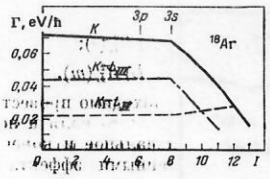

FIG. 16. Changes in the total probability of K transitions and the probabilities of K_{α_1} (K–L_{III}) and K_{α_2} (K–L_{II}) transitions following ionization of the outer shell of argon, calculated for the ground states of the ions; I is the degree of ionization, and the completely stripped shells are indicated at the top.

changes in the probabilities of K–L_{II} and K–L_{III} (K_{α_2} and K_{α_1}) transitions in the case of successive ionization of outer electrons in the atomic shell of Ar are shown in Fig. 16. In the case of ionization of outer electrons, the probabilities of K_α transitions and the total probability of K transitions change little. Only ionization of electrons in the L shell has an influence. The influence of additional vacancies in the inner shells of the atom is shown in Fig. 17 for the example of the total probability of K transitions in the presence of additional vacancies in the $2p$ and $3p$ shells in the ground states of the Ar ions.[97] The results in Fig. 17 are obtained on the basis of wave functions calculated by the Hartree–Fock–Slater method. Additional vacancies in the $2p$ shell have a much stronger influence on the probabilities of x-ray K transitions than vacancies in higher shells. This corresponds to the intensity distribution within the K series; the K_α transitions (K–L_{II}, L_{III}) are the most intense. On the removal of electrons from the $2p$ level, the ratio K_β/K_α increases appreciably, which is explained by the decrease in the number of electrons participating in the K_α transitions. The removal of electrons from higher levels with the number of electrons in the $2p$ level remaining the same leads to a decrease in the K_β/K_α ratio. The relative intensities of the x-ray satellite lines are determined by the distribution of the atoms over the possible states. If the system is in dynamical equilibrium and the number of atoms in the different states of a configuration is the same, the number $n(f|ij)$ of quanta for transitions between all states j with vacancy i in configuration f is

$$n(f|ij)=\frac{\Gamma^R(f|ij)}{\Gamma(ij)}\left[P(ij)N_i+\sum_{kl>ij}W(ij|kl)N'(kl)\right],$$

where $\Gamma(ij)$ and $\Gamma^R(f|ij)$ are the total probabilities of decay and radiative decay of configuration (ij); $P(ij)$ is the relative probability of formation of atoms with configuration (ij); N_i is the number of atoms with vacancy that are formed as a result of direct ionization. The sum in the brackets takes into account the formation of atoms of configuration (ij) from (kl), where in the relative probability $W(ij|kl)$ of transition of atoms of configuration (kl) allowance is made for all radiative and nonradiative transitions that carry the configuration (kl) to (ij).[1)]

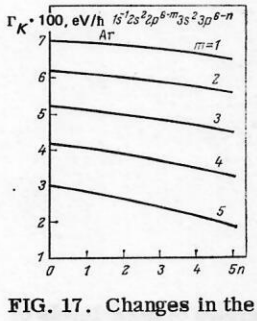

FIG. 17. Changes in the total probability of x-ray K transitions of Ar in the presence of additional vacancies in the $2p$ and $3p$ shells.[97]

3. ELECTRON BINDING ENERGIES OF IONIZED ATOMS

Figures 1–7 give examples of the energy shifts of x-ray lines following ionization of atomic shells. These shifts are due to the decrease in the screening and the associated increase in the electron binding energy. The binding energy changes in different ways for different levels. The energy separation between the electron states changes, which is manifested in the energy shifts of the corresponding x-ray transitions. In Ref. 100, the Dirac–Fock–Slater method is used to calculate the binding energies for all levels and all degrees of ionization of xenon. In Ref. 101, these quantities are calculated for U. The shifts of the binding energies for some electron states and degrees of ionization of neptunium are also calculated by the Dirac–Fock–Slater method in Ref. 189. For neon ions, corresponding data obtained by the Hartree–Fock method are contained in Ref. 190. The ionization potentials of an outer electron for all ground states of ions up to $Z = 103$ are given in Ref. 191. The experimental values of the ionization potentials obtained by analysis of optical spectra are given in Refs. 192–196. Theoretical values for the first 36 elements, corrected with allowance for the experimental data of Refs. 192–195, are given in Ref. 197.

The experimental ionization potentials[194, 195] are compared with the calculated potentials in Table VIII. The calculations were made by the Dirac–Fock–Slater method. The table shows the accuracy with which the ionization potentials can be determined in the framework of this method. Allowance for further corrections (electron correlations, quantum-electrodynamic effects; see Sec. 1) increases the accuracy of the calculations.

In Ref. 198, the ionization potentials are determined for the chemical elements with serial numbers 71–86 and 81–102 for electrons of the O and P levels. A diagram of the binding energies of electrons of the K, L, M, N, O, P, Q levels is constructed for all elements of the periodic table.

When an electron is removed by ionization, the total potential in the atom V_{HF} ($V_{HF} = V_C + V_S$, where V_C is the Coulomb potential of the nucleus, and V_S is the po-

[1)] There is much detailed information about the intensities of radiative transitions of electrons of outer shells for neutral atoms and atoms in low ionization states. Unfortunately, there is very little information about the influence of the multiplicity of ionization on the radiative transitions in inner atomic shells. Here we need extensive theoretical and experimental investigations in order to clarify the physical picture of the phenomena of interest for diagnostics of a thermonuclear plasma and astrophysical investigations.

TABLE VIII. Comparison of experimental values of ionization potentials[194,195] with values calculated by the Dirac–Fock–Slater method. (I is the degree of ionization, E_{exp} are the experimental energies, and E_{DFS} are the calculated values).

Calcium, $Z=20$			Manganese, $Z=25$		
I	E_{exp}, eV	E_{DFS}, eV	I	E_{exp}, eV	E_{DFS}, eV
0	6.1	5.4	0	7.4	7.2
1	11.9	11.7	1	15.6	14.9
3	67.3	66.7	6	119.3	117.5
5	108.8	104.1	13	404.0	404.3
7	147.6	145.7	14	435.3	437.8
9	211	212.7	15	1136.2	1129.8
11	657	657.3	21	1765.5	1784.2
13	818	802.6	23	8082.5	8122.5
15	974	961.4	24	8571.5	8575.6
Gallium, $Z=31$			Lead, $Z=82$		
0	6.0	5.0	0	7.4	6.4
1	20.5	19.9	1	15.0	14.0
2	30.7	30.6	2	31.9	31.9
3	68	62.4	3	42.3	42.1
4	90	87.0	4	68.8	68.4

tential of the self-field of the electrons) changes; as a rule, the contribution V_s decreases. The screening potential can be written in the form[199]

$$V_S(\mathbf{r}) = \int \rho(\mathbf{r})' \, d^3r' / |\mathbf{r} - \mathbf{r}'|,$$

where $\rho(\mathbf{r})$ is the density of the electron charges. Removal of an electron from the atom leads to a change $\delta\rho(\mathbf{r})$ of the charge density. The change in the screening is

$$\delta V_S(\mathbf{r}) = \int \delta\rho(\mathbf{r}') \, d^3r' / |\mathbf{r} - \mathbf{r}'|.$$

In the first order of perturbation theory, the energy shift of the corresponding electron level is

$$\Delta E = \int \frac{\delta\rho(\mathbf{r}')\,\rho(\mathbf{r})}{|\mathbf{r}-\mathbf{r}'|} d^3r' \, d^3r.$$

Calculations show[100,101] that the changes ΔE in the binding energy following ionization with removal of one valence electron are of order 10 eV. The results of calculations of the change in the binding energy following removal of a valence electron are shown in Fig. 18, from which it can be seen that the change in the binding energy depends on the electron configuration. Within each period of the periodic table the shifts of the electron binding energies increase, since the charge of the nucleus increases and the electrons fill the same shell. The smallest shifts are observed for the alkali metals, while the noble gases with electron configuration ns^2np^6

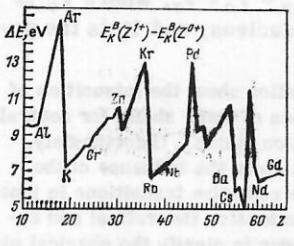

FIG. 18. Changes in the binding energy ΔE_K of electrons of the K shell resulting from the removal of one valence electron, calculated by the Dirac–Fock–Slater method.

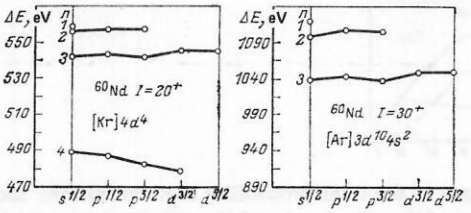

FIG. 19. Differences between the binding energies of the neutral atom and Nd ions. Calculations by the Dirac–Fock–Slater method.

have the largest shifts of the binding energies. For the elements of one principal group the change in the binding energy decreases on the transition to higher periods. This is explained by the fact that with increasing number of the period the outer electron shell is further from the nucleus.

For a detailed demonstration, Fig. 19 shows the differences between the binding energies for different subshells of the neutral atom and some Nd ions. Usually, the change in the binding energy is greatest for the inner levels, since the reduction in the screening is here very appreciable. The removal of electrons with high angular momenta has less influence on the screening of the K-shell electrons than it does on the higher levels. Therefore, the change in the binding energy of the K-shell electrons with increasing ionization may become less than for the higher levels, which is the reason for the negative x-ray energy shifts. This effect is manifested only in the inner shells, and negative energy shifts of x-ray transitions are not observed for the M series. The changes in the binding energies of the K level of noble gases up to Xe are shown in Fig. 20. Large changes in the binding energy are observed when electrons are removed from the ns shells, which is due to the concentration of these electrons near the nucleus and their strong influence on the screening of the remaining electrons.

The numerical values of the first ionization potentials are given for all elements of the periodic table in Ref. 95. The information given there was obtained primarily by analyzing series of optical transitions induced by various excitation sources. At the present time there are almost no experimental data for different charge states of ions. The only possibility of finding electron

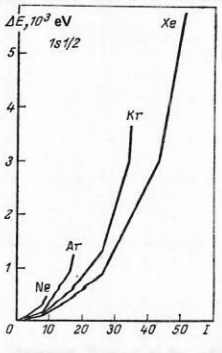

FIG. 20. Changes in the binding energies of the K levels of noble gases, calculated for the ground states I of the ions. Calculations by the Dirac–Fock–Slater method.

binding energies in a large region of states is by self-consistent field calculations. For exact calculations of the binding energies of inner electrons it is necessary to take into account the effects of magnetic interaction, retardation, and quantum-electrodynamic corrections (see Sec. 1).

4. NONRADIATIVE TRANSITIONS

The importance of nonradiative transitions

Most studies of nonradiative transitions have been of neutral atoms. Hitherto, processes with a small number of vacancies in the atomic shell have been of practical interest. Nonradiative transitions are basically used for detailed investigation of wave functions. Because of the high sensitivity of nonradiative transitions to the form of the wave functions, the obtained information is used to improve the existing numerical methods of calculating wave functions. Detailed knowledge of the probabilities and energies of nonradiative transitions is needed to interpret many measurements in nuclear and atomic physics. Especially important is the x-ray fluorescence yield, from which the ionization cross section is determined. The fluorescence yield ω_i is the probability that after ionization in state i an x-ray photon is emitted. The ionization cross section σ_i^I for state i can be determined from the total cross section σ_i^R of the x-ray transition or from the cross section σ_i^A for emission of Auger electrons:

$$\sigma_i^I = \sigma_i^R/\omega_i = \sigma_i^A/(1-\omega_i).$$

The fluorescence yield and the probabilities of Auger and Coster–Kronig processes for neutral atoms are given in Ref. 51. Of great interest are investigations of the nonradiative process of multiplication of vacancies formed in the inner shells of atoms—the so-called *Auger cascades*. The Auger effect in an inner shell of an atom leads to double ionization, and successive nonradiative transitions may lead to multiple ionization.

The fluorescence yields have great importance in many applied problems, for example, in x-ray spectral analysis (analysis of the chemical composition in industry, medicine, and geology) and in problems of radiation protection (description of photon transport processes on the basis of the Boltzmann equation, for example).

There are three main possibilities for filling inner vacancies accompanied by electron emission.

The Auger effect[149,150]: the filling of an inner vacancy with emission of an electron and transitions in which a vacancy in one shell of an atom leads to two vacancies in one or two other principal shells.

In *Coster–Kronig transitions*[122] a nonradiative transition results in one of two vacancies that are formed being in a different subshell of the same principal shell from the primary vacancy.

Super-Coster–Kronig transitions[176] correspond to the situation when a primary vacancy leads to two vacancies in subshells of one principal shell.

Analysis of the existing material on Auger transitions shows that the calculated and experimental data are in satisfactory agreement. The discrepancies between experiment and theory in some parts of the periodic table can be reduced by a further experiment or by more accurate numerical values of the calculated functions. There is almost no experimental information about nonradiative transitions in multiply ionized atoms, and calculated results are also very sparse. In principle, the quantities one needs can be obtained by taking wave functions from self-consistent calculations and using the matrix elements for nonradiative transitions from Ref. 32. In the theory of satellites and Auger hypersatellites few numerical results have yet been obtained. There have been measurements of complicated Auger spectra produced by ion–atom collisions.[200,201] It was found that satellites that are weak compared with the main Auger lines for electron or photon excitation can become the dominant lines in the case of ion–atom collisions.

In what follows, we give a general scheme for calculating the energy and intensity of nonradiative electron transitions in the presence of vacancies in the configuration. We give some numerical results to illustrate the significance of the various effects.

Energies of nonradiative electron transitions in multiply ionized atoms

As we pointed out above, there is almost no experimental information about the energies of nonradiative transitions. The energies of the corresponding transitions can be calculated. For the Auger process ($W_i - X_jY_k$) the transition energy is determined by the expression

$$E(W_i - X_jY_k) = E_{\text{exc}}[W_i] - E_{\text{exc}}[X_jY_k],$$

or

$$E(W_i - X_jY_k) = \varepsilon_B^Z(W_i) - \varepsilon_B^Z(X_j) - \varepsilon_{Y_k}^Z[X_j],$$

or

$$E(W_i - X_jY_k) = \varepsilon_B^Z(W_i) - \varepsilon_B^Z(Y_k) - \varepsilon_{X_j}^Z[Y_k],$$

where $\varepsilon_B^Z(X_i)$ is determined by Eq. (12); $\varepsilon_{Y_k}^Z[X_j]$ is the binding energy of the electrons in subshell Y_k of the initial atom with atomic number Z, which has a vacancy in subshell X_j.

To determine the energies of Auger transitions in atoms without additional vacancies, use is made of empirical and semiempirical rules,[82] which require knowledge of the binding energies of the electrons that participate in the transitions. The use of this technique is restricted in the determination of satellite energies by the fact that in the majority of cases the corresponding experimental electron binding energies are not available. Relativistic self-consistent calculations are often used to determine the energies of nonradiative transitions. The reviews of Refs. 32 and 82 are devoted to the technique of such calculations.

As an example, Fig. 21 gives the energy shifts of some lines of the K series for the ground states of Nd ions. The calculations were made by Dirac–Fock–Slater method. We note that for the Auger and Coster–

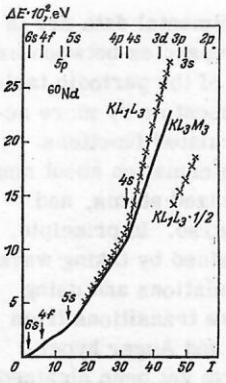

FIG. 21. Dependences of the energy shifts of the K lines of Auger transitions for Nd on the number of outer vacancies I calculated by the Dirac–Fock–Slater method. The completely stripped shells are indicated at the top.

Kronig transitions there are energy restrictions. With increasing degree of ionization, the energy reserves of the atomic levels may change in such a way that the differences between the binding energies of the electrons that participate in the transition are not sufficient for removal of an additional electron.[100]

Calculations show that, in contrast to Coster–Kronig transitions, only filling of the outer orbitals by electrons is necessary for Auger transitions of the K and L series. Additional internal vacancies have little influence on the energies of the atomic shells and must be investigated specially in each particular case.

Intensities of nonradiative electron transitions in multiply ionized atoms

The foundations of the quantum-mechanical treatment of nonradiative transitions were laid by Wentzel.[202] The nonrelativistic probability of transition per unit time is[203]

$$W_{fi}=2\pi\left|\left\langle\psi_a\psi_b\left|\frac{1}{|\mathbf{r}_1-\mathbf{r}_2|}\right|\psi_c\psi_d\right\rangle_A\right|^2, \tag{18}$$

where ψ_c is a continuum wave function; ψ_a, ψ_b, and ψ_d are bound-state wave functions. The subscript A indicates that the matrix element is calculated with antisymmetric wave functions in the initial and final states. The function ψ_c is normalized to unity.

Using the atomic unit of energy $e^2/a_0 = 27.2116$ eV and measuring distances in Bohr radii a_0, we write (18) in the form

$$W_{fi}=2\pi\frac{e^2}{\hbar a_0}\left|\left\langle\psi_i\left|\frac{1}{|\mathbf{r}_1-\mathbf{r}_2|}\right|\psi_f\right\rangle_A\right|^2=\frac{2\pi}{5}\left|\left\langle\psi_i\left|\frac{1}{|\mathbf{r}_1-\mathbf{r}_2|}\right|\psi_f\right\rangle_A\right|^2.$$

The atomic unit of time $\tau=\hbar a_0/e^2=\hbar^3/me^4=2.42\times10^{-17}$ sec is the unit of measurement of the transition probability. An excited state decays with probability $\sum_f W_{fi}$. The mean lifetime of the state is $T=1/\sum_f W_{fi}$, and in accordance with the uncertainty principle the effective width of the line is $\Delta E=\hbar/\tau=\hbar\sum_f W_{fi}$. In the relativistic variant of the calculation,[204] the expression (18) is rewritten as

$$W_{fi}=2\pi\,|\,\langle\psi_a\psi_b\,|\,V(12)\,|\,\psi_c\psi_d\rangle_A\,|^2.$$

The perturbing interaction is represented in the state-dependent form[205] (in atomic units)

$$V_\omega=(1-\alpha_1\alpha_2)\exp(i\omega r_{12})/r_{12}, \tag{19}$$

where $\omega=|E_c-E_a|/c=|E_d-E_b|/c$. Here, $E_{a,b,c,d}$ are energy eigenvalues of the orbitals a, b, c, and d. The interaction is determined by exchange of a virtual photon between two electrons in quantum electrodynamics and includes the Breit interaction and the Coulomb interaction. The expression (19) is valid only for electron orbitals in a local potential (Dirac–Fock–Slater method). In the Dirac–Fock model, the nonlocal generalization of this potential has the form[204]

$$V_\omega(12)=\frac{1}{r_{12}}-(\alpha_1\alpha_2)\frac{\exp(i\omega r_{12})}{r_{12}}+(\alpha_1\nabla_1)(\alpha_2\nabla_2)\frac{\exp(i\omega r_{12})-1}{\omega^2 r_{12}} \tag{20}$$

in the integral form proposed by Bethe and Salpeter.[206] The first term of the expression (20) describes the Coulomb interaction between the charges; the second, the retarded interaction between the currents; and the third takes into account the correction for retardation in the Coulomb interaction. The retardation is taken into account by the scalar Green's function $\exp(i\omega r_{12})/r_{12}$. The retardation effects are negligibly small if the radii of the corresponding atomic subshells are much less than the wavelength $\lambda=2\pi c/\omega$, which is so in the majority of cases.

In the relativistic approach, one is recommended to take into account jj coupling. When the Coulomb interaction is predominant, practical calculations are made in the nonrelativistic approximation. To estimate the influence of the individual terms in (20) on the accuracy of the calculations, we transform (20) to the form[204]

$$V_\omega(12)=\frac{1}{r_{12}}-(\alpha_1\alpha_2)\frac{1}{r_{12}}\left[\exp(i\omega r_{12})\left(1+\frac{i}{\omega r_{12}}-\frac{1}{\omega^2 r_{12}^2}\right)+\frac{1}{\omega^2 r_{12}^2}\right]+(\alpha_1 r_{12})(\alpha_2 r_{12})\frac{1}{r_{12}^3}\times\left[\exp(i\omega r_{12})\left(1+\frac{3i}{\omega r_{12}}-\frac{3}{\omega^2 r_{12}^2}\right)+\frac{3}{\omega^2 r_{12}^2}\right].$$

In the long-wave approximation,

$$V_\omega(12)=\frac{1}{r_{12}}-\frac{1}{2r_{12}}[(\alpha_1\alpha_2)+(\alpha_1 r_{12})(\alpha_2 r_{12})/r_{12}^2]-\frac{2i}{3}\omega(\alpha_1\alpha_2)+O(\alpha_1)(\alpha_2)(\omega r_{12})^2. \tag{21}$$

For atoms with $Z<40$, the nonrelativistic treatment using the Coulomb potential gives an accuracy of about 1%. The corresponding results for the outer shells of heavy elements are given by relativistic calculations including the Breit interaction in the range $40\leq Z\leq 70$ [order $(Z^*\alpha)^2$ relative to the Coulomb interaction, where Z^* is the effective charge]. For elements in the range $70\leq Z\leq 90$ it is necessary to take into account the third term in (21), which gives a correction of order $(Z^*\alpha)^3$. If Z exceeds 90, then it is necessary to take into account fully all the terms in (20). The correction here is of order $(Z^*\alpha)^4$.

Satellite lines in Auger spectra were first observed[207] in 1966 and since then have been widely studied. Examples can be found for Ne in Ref. 208 and Kr and Xe in Ref. 209.

The method of calculating the probability of the Auger effect applies to atoms containing different vacancy distributions, i.e., it is in principle possible to make calculations for multiply ionized ions. However, much

TABLE IX. Transition probabilities (in atomic units) for Auger transitions of argon.

Transition	$m=5$		$m=4$		$m=3$		$m=2$		$m=1$	
	A	B	A	B	A	B	A	B	A	B
$2p-3s3s$	17.2	21.8	18.3	21.8	19.9	21.8	21.9	21.8	23.9	21.8
$2p-3s3p$	291.1	293.9	252.0	234.6	209.2	175.8	152.9	117.0	83.8	58.5
$2p-3p3p$	735.7	870.7	500.7	522	285.7	261.8	108.3	87.3	0.0	0.0
Полная вероятность	1061.2	1186	770.0	778.2	514.3	459.8	283.0	226.1	107.8	80.3

Note. A) Quantum-mechanical calculations[210] for the configurations $(1s^22s^22p^53s^23p^m3d^1)$; B) calculated values of the configurations $(1s^22s^22p^63s^23p^m)$ obtained by Larkins's method.[162]

must still be done to obtain a complete picture of the corresponding quantities for different configurations with vacancies. Table IX contains the probabilities of Auger transitions for different configurations of outer vacancies in Ar. Besides the results obtained by the self-consistent field method, we give results found by Larkins's method.[162] The results of the two methods of calculation differ by 25%.

The fluorescence yields of the K shell of Ar in the presence of additional vacancies are given in Fig. 22. The bound-state wave functions were calculated by the Hartree–Fock–Slater method. The use of the simpler procedure of Larkins gives the same qualitative behavior of the fluorescence yield, but overestimates the results by 25%. The difference between the results is explained by the fact that in Larkin's approximate procedure no allowance is made for the changes in the transition energies and the wave functions for electron defect configurations. Knowledge of the probabilities of Auger transitions in a multiply charged atom makes it possible to calculate the corresponding fluorescence yields and to use them to determine the cross sections of multiple ionization of atoms and ions.

5. IONIZATION OF ATOMS AND IONS

Multiple ionization is observed in collisions of particles with atoms or ions or in the process of rearrangement of atomic shells when inner vacancies are filled. In a collision, there are appreciable probabilities for both instantaneous formation of a multiply ionized atom and the formation of a primary vacancy followed by Coster–Kronig transitions and Auger cascades. To determine the characteristic time of formation of n-fold charged positive ions in, for example, intense electron beams of electron-beam ion sources[211] and in electron–ion rings of collective heavy-ion accelerators,[13] it is necessary to know the cross section of direct and multiple indirect ionization. Analysis of the ionization process of atoms in plasma sources makes it possible

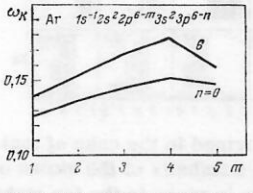

FIG. 22. Change in the fluorescence field of the K shell of Ar for different vacancy configurations.[97]

to choose the optimal regime of operation of such sources.

The ionization of atoms by light (electrons, γ rays) and heavy particles is basically different. The ionization by light particles is characterized by the formation of one or several primary vacancies; in the case of ionization by heavy particles, the vacancy distribution is much more complicated.

In collisions of atoms with heavy particles, electrons are knocked out with definite probability from different subshells of the atom and an ion with definite ionization multiplicity is obtained. As a rule, development of the process in the direction of further ionization is already impossible. In ion sources of the electron-beam type or in the electron rings of a collective heavy-ion accelerator the situation is different. Here, the ionization develops in time. The attained degree of ionization depends on the specific parameters of the source and on the time during which the atom remains in the ionizing medium. Since this process is of great interest for a number of applications, we shall dwell on it here in more detail.

Ionization processes in ion–atom collisions are considered in Ref. 156. The ionization of inner shells due to the Coulomb interaction with incident particles is calculated in various approaches. The most important methods of approximate calculations of Coulomb ionization processes are the following: a) the plane-wave Born approximation[212-215]; b) the quasiclassical approximation[216]; c) the classical two-center approximation.[217-222]

The regions of applicability of these approximations are discussed in detail in Ref. 132. For $Z_1 \approx Z_2$ (Z_1 is the atomic number of the incident particle, Z_2 that of the target atoms) and velocities v_p of the incident particles small compared with the electron orbital velocity v_e the molecular-orbital method (MO method)[132] can be used to describe ionization processes in inner atomic shells. In accordance with this model, an electron from the inner shells goes over to a higher state as a result of the interaction of the overlapping molecular orbitals. Such a process is possible only when the binding energies of the corresponding orbitals are equal or nearly so. In the case of slow collisions ($v_e \gg v_p$), the reaction cross section given by the MO model is several orders larger than the cross section of direct Coulomb ionization. In order of magnitude, the cross section for ionization by heavy ions is 10^4–10^7 b and depends on the atomic number and energy of the incident particle. For protons and α particles, the ionization cross section is 10^1–10^4 b, depending on the energy of the incident particle.

Calculations have been made of the ionization cross sections of atoms bombarded with relativistic (see Refs. 14, 15, 223, and 224) and nonrelativistic electrons.[225-232] There have been relatively few calculations for relativistic electron energies, since the nonrelativistic energy region has long been the main interest. Up to the present time, the ionization cross sections of ions have been measured mainly by the method of inter-

secting electron and ion beams.[233] This method has a good energy resolution for low ion charge states. Therefore, only processes with the participation of doubly and triply charged ions have been investigated.[234,235] Highly charged ions were investigated using a Penning ion source by Crandall[236,237] in 1979. Donets *et al.*[238,239] succeeded in measuring the ionization cross sections of ions of high charge states using an electron-beam source.[240-242]

Most calculations in the nonrelativistic region of electron energies are made using Thomson's classical expression for the ionization cross section[243]:

$$\sigma(E)=6.5\cdot10^{-14}\sum_j\frac{n_j}{I_jE}\left(1-\frac{I_j}{E}\right),$$

where $\sigma(E)$ (cm^2) is the total ionization cross section, E (eV) is the collision energy, n_j is the number of electrons in subshell j, and I_j (eV) is the binding energy in this subshell.

When quantum mechanics was developed, the behavior of the ionization cross section at high energies was clarified. The energy dependence of the cross section has the form $\log(E)/E$. To determine the ionization cross sections with allowance for the electron binding energy and the correct asymptotic behavior, Lotz's semi-empirical expression is widely used[228,244]:

$$\sigma(E)=4{,}5\cdot10^{-14}\sum_j\frac{n_j}{I_jE}\ln\left(\frac{E}{I_j}\right). \qquad (22)$$

This expression is valid for ions with charge greater than +3. For ions with charge less than 3, the expression (22) gives the results that are closest to the experimental results, but this good agreement is in no way rigorously justified and appears to be fortuitous. The most correct description of ionization by electron impact is given by the Coulomb–Born method.[245-246] The Born transition amplitude is calculated as an integral of the product of the wave functions of the initial and final states and the interaction potential of the system. Difficulties and further approximations are associated with the particular choice of the wave functions and allowance for the exchange interaction. Corresponding calculations have been made only for hydrogenlike ions[226,245] and for some cases of interest for comparing the results of experiment and theory.

The ionization cross section obtained by the Coulomb–Born method with allowance for exchange[231,247-250] for hydrogenlike ions up to configurations with $4f$ subshells has the form

$$\sigma(E)=\pi a_0^2\sum_j\left(\frac{n}{Z_{\text{eff}(j)}}\right)^2\frac{I_H}{I_j}\frac{n_j}{\mu_j}\left[A_j\ln\mu_j+D_j\left(1-\frac{1}{\mu_j}\right)^2+\left(\frac{c_j}{\mu_j}+\frac{d_j}{\mu_j^2}\right)\left(1-\frac{1}{\mu_j}\right)\right]; \qquad (23)$$

here, n is the principal quantum number of level j, I_H = 13.6 eV, $\mu_j = E/I_j$, $Z_{eff}(j)$ is the effective charge of the nucleus of the initial ion, and A_j, D_j, c_j, and d_j are numerical coefficients given in Refs. 231 and 247–249. The expression (23) is physically very well founded, but it agrees less well than Lotz's expression (22) with the experimental data. The results of experiments with intersecting beams indicate that (23) is not accurate when the excitation–autoionization process plays an important part. Allowance for an approximate contribution of this process improves (23).

Calculations by Burgess's method[250,251] give better agreement with the experiments for singly and doubly charged ions than the empirical expressions of Ref. 252. In Burgess's method, allowance is made for the exchange interaction of collisions with large impact parameters. In future, particular attention must be paid to the development of models that take into account the excitation–autoionization process. The cross sections for ionization of ions by relativistic electrons are almost unknown. This problem has been the subject of a few studies (Refs. 14, 15, 223, 224, 253, and 254) in connection with the development of heavy-ion accelerators. In Refs. 224 and 253 there are estimates of the ionization cross sections for electrons of the inner shells on the basis of a single-particle model.[255] The ionization cross sections contain contributions from direct ionization and Auger transitions. The calculations are only approximate, but they do allow one to estimate the ionization cross sections for different Z and degrees of ionization of the atom, which is needed in the development of sources of heavy-ion accelerators.

Salop[14,15] calculated the total ionization cross sections and cross sections of multiple ionization of noble gases up to Xe. Total ionization cross sections were calculated in the Bethe–Born approximation.[203,256]

Rearrangement processes in the atomic shell in the presence of inner vacancies lead to the emission of one or several electrons in Auger transitions or to the shake-off effect. For vacancies in the (n, l) subshell one can determine the probability of emission of j electrons, including the primary electron: $S^I_{nl}(j)$. If it is assumed that the rearrangement following the formation of a vacancy and the transition of an electron to a higher level is the same as for direct ionization, then the probability of emission of electrons following excitation is

$$X^I_{nl}(j)=S^I_{nl}(j+1)\Big/\sum_{k=2}^{m}S^I_{nl}(k),\quad j>0,$$

where m is the maximal possible number of electrons that can be removed from the ion. The cross section of

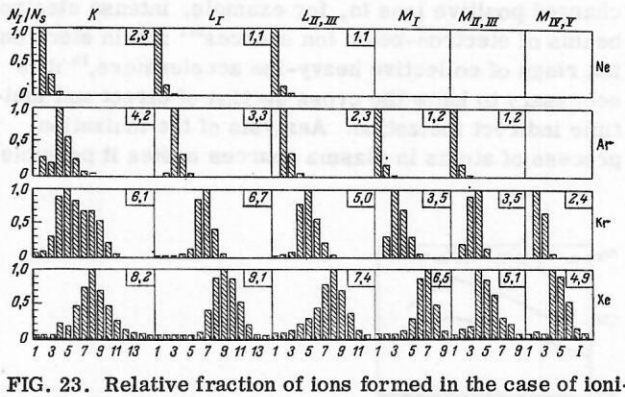

FIG. 23. Relative fraction of ions formed in the case of ionization by photons from the different subshells of the atoms of the noble gases.[257] The mean charge is given in the top right-hand corner; I is the degree of ionization.

TABLE X. Cross sections of j-fold ionization of ions of charge I of krypton by 20-MeV electrons[14] (in cm^2).

I	$j=1$	2	3	4	5	6
0	9.14 (—19)	3.03 (—19)	1.18 (—19)	2.36 (—20)	4.44 (—21)	1.27 (—21)
1	1.81 (—19)	1.71 (—19)	1.11 (—19)	2.05 (—20)	3.88 (—21)	1.21 (—21)
2	9.70 (—20)	1.47 (—19)	9.81 (—20)	1.85 (—20)	3.53 (—21)	1.16 (—21)
3	9.60 (—20)	1.34 (—19)	8.00 (—20)	1.68 (—20)	3.27 (—21)	1.11 (—21)
4	1.87 (—19)	9.98 (—20)	3.72 (—21)	3.34 (—21)	—	—
5	2.09 (—19)	5.44 (—20)	3.09 (—21)	—	—	—
6	2.00 (—19)	4.36 (—20)	2.88 (—21)	—	—	—

multiple ionization following the formation of an ion with charge $I_F = I + j$ from an ion with charge I as a result of an electron–ion collision is

$$\sigma^M(I,\ I_F) = \sum_{nl} \sigma^C_{nl}(I)\, S^I(j) + \sum_{nl} \sigma^A_{nl}(I)\, X^I_{nl}(j),$$

where $\sigma^C_{nl}(I)$ is the cross section for ionization of the ions in the charge state I by electrons for direct transitions to the continuum and $\sigma^A_{nl}(I)$ is the corresponding cross section for excitation of the electrons.

There is almost no experimental information about the functions S^I_{nl} and X^I_{nl}. The only experimental results were obtained by Carlson *et al.*[257] The relative fractions of ions formed following photoionization of neutral atoms of the noble gases are shown in Fig. 23. A detailed estimate of the functions S^I_{nl} and X^I_{nl} is described in Refs. 14 and 15.

We note that for ions with a low charge state the cross sections of j-fold ionization may exceed the direct-ionization cross sections. The behavior of the multiple-ionization cross sections is illustrated for krypton in Table X.

The results of calculations by Salop's method are demonstrated in Fig. 24 (for Kr). It can be seen that the contribution to the ionization cross section of nonradiative processes can exceed the direct-ionization contribution in some ranges of the multiplicity of ionization of the atom.

The direct-ionization cross section is calculated using hydrogen-like wave functions in Ref. 258 and in the generalized Kolbenstved model.[223] Both the quoted studies give cross sections that exceed Salop's results. It is difficult to estimate the accuracy of the calculations because of the lack of experimental material.

Since there is as yet very little experimental information about the ionization cross sections of highly ionized atoms, it is difficult to draw conclusions that would stimulate theory to the improvement of the existing approximate methods of calculation.

CONCLUSIONS

The vigorous development of heavy-ion accelerators and the associated heavy-ion sources, the mastering of the fundamentals of controlled thermonuclear fusion, and progress in astrophysical investigations make it essential for us to know the structure of highly ionized ions and the processes in the atomic shells of such ions. It is necessary to know how the parameters of the radiative and nonradiative processes, the energy structure of the atomic shells, and the ionization cross sections vary with increasing degree of ionization of the atoms.

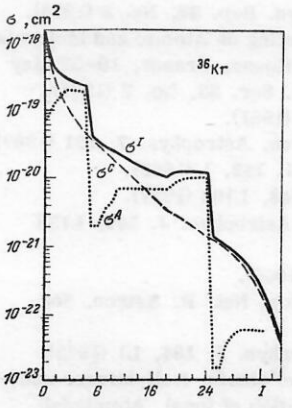

FIG. 24. Cross section for ionization of Kr by 20-MeV electrons for the ground states of the ion: σ^I is the total ionization cross section, σ^C is the direct-ionization cross section, and σ^A is the ionization cross section due to nonradiative processes; I is the degree of ionization.

At the present time, there is hardly any experimental information on highly ionized atoms. In the literature there are only ionization potentials for the outer electrons of light ions and some weakly ionized heavy ions,[196-200] and the energy shifts of the characteristic x-ray lines are known for a number of chemical compounds and for atoms with additional vacancies in the inner shells. Except for investigations for some ions and certain vacancy distributions, experimental information is almost completely absent for a large number of configurations with vacancies.

To obtain a picture of the variations and order of magnitude of the important parameters for different states of the atoms in the presence of vacancies, calculations of the structures and processes have hitherto been used in the majority of cases. The results found by calculation have not been verified experimentally. Our knowledge about the processes and structures of highly ionized atoms has been obtained from models developed, as a rule, on the basis of analysis of processes in neutral or weakly ionized atoms. Therefore, besides the improvement of the existing algorithms and models, it is necessary to make experimental studies of the structure of multiply charged ions and the interactions in them. Valuable means for this are the unique sources of multiply charged ions such as the electron–ion rings of a collective heavy-ion accelerator, electron-beam sources, and some other facilities. Such sources make it possible to carry out systematic investigations of ions of different elements in a wide range of charge states.

I am grateful to Professor G. Muziol and Dr. É. A. Perel'shteĭn for helpful discussions during the preparation of this review.

[1]IAEA Advisory Group Meeting on Atomic and Molecular Data for Fusion, held at the UKAEA Culham Laboratory, Abingdon, U.K., 1–5 November (1976); Proc. issued as Technical

Document IAEA-199 (1977); Phys. Rep. **37**, No. 2 (1978).
[2]Second Technical Committee Meeting on Atomic and Molecular Data for Fusion, Fontenay-aux-Roses, France, 19–22 May (1980); Proc. published in Phys. Scr. **23**, No. 2 (1981).
[3]D. Palumbo, Phys. Scr. **23**, 69 (1981).
[4]W. M. Neupert, Ann. Rev. Astron. Astrophys. **7**, 121 (1969).
[5]R. L. Blake *et al.*, Astrophys. J. **142**, 1 (1965).
[6]G. Fritz *et al.*, Astrophys. J. **148**, L133 (1967).
[7]R. L Blake and L. L. Hauser, Astrophys. J. **149**, L133 (1967).
[8]L. W. Acton, Nature **207**, 737 (1965).
[9]A. H. Gabriel and C. Jordan, Mon. Not. R. Astron. Soc. **145**, 241 (1969).
[10]P. J. Serlemitsos *et al.*, Astrophys. J. **184**, L1 (1973).
[11]V. P. Sarantsev and É. A. Perel'shteĭn, Kollektivnoe uskorenie ionov (Collective Acceleration of Ions), Atomizdat, Moscow (1979).
[12]G. Zschornack, G. Müller, and G. Musiol, Nucl. Instrum. Methods **173**, 457 (1980).
[13]D. Lemann *et al.* Preprint 9-10744 [in Russian], JINR, Dubna (1977).
[14]A. Salop, Phys. Rev. A **8**, 3032 (1973).
[15]A. Salop, Phys. Rev. A **9**, 2496 (1974).
[16]F. Herman and S. Skillman, Atomic Structure Calculations, Prentice-Hall, Englewood Cliffs, N. J. (1963).
[17]D. A. Liberman, J. T. Waber, and D. T. Cromer, Comput. Phys. Commun. **2**, 107 (1971).
[18]A. Rosén and I. Lindgren, Phys. Rev. **176**, 114 (1968).
[19]C. C. Lu *et al.*, At. Data Tables **3**, 1 (1971).
[20]S. Fraga, J. Karwowski, and K. M. S. Saxena, Handbook of Atomic Data, Elsevier, New York (1976).
[21]C. Froese-Fischer, Comput. Phys. Commun. **14**, 145 (1978).
[22]M. A. Coulthard, Proc. Phys. Soc. London **91**, 44 (1967).
[23]F. C. Smith and W. R. Johnson, Phys. Rev. **160**, 136 (1967).
[24]J. B. Mann, J. Chem. Phys. **51**, 841 (1969).
[25]J. P. Desclaux, D. F. Mayers, and F. O'Brien, J. Phys. B **4**, 631 (1971).
[26]I. Lindgren and A. Rosen, Case Stud. At. Phys. **4**, 93 (1974).
[27]J. P. Desclaux, Comput. Phys. Commun. **9**, 31 (1975).
[28]I. P. Grant *et al.*, Comput. Phys. Commun. **21**, 207 (1980).
[29]J. C. Slater, Phys. Rev. **81**, 385 (1951).
[30]B. J. McKenzie, I. P. Grant, and P. H. Norrington, Comput. Phys. Commun. **21**, 233 (1980).
[31]J. H. Scofield, "Radiative transitions," in: Atomic Inner-Shell Processes, Vol. 1, Academic Press, New York (1975), p. 265.
[32]E. J. McGuire, "Auger and Coster–Kronig transitions," in: Atomic Inner-Shell Processes, Vol. 1, Academic Press, New York (1975), p. 293.
[33]D. H. Madison and E. Merzbacher, "Theory of charged-particle excitation," in: Atomic Inner-Shell Processes, Vol. 1, Academic Press, New York (1975), p. 2.
[34]E. A. Hylleraas, Z. Phys. **54**, 347 (1929).
[35]C. L. Pekeris, Phys. Rev. **112**, 1649 (1958).
[36]D. R. Hartree, Proc. Cambridge Philos. Soc. **24**, 89 (1927).
[37]D. R. Hartree, The Calculation of Atomic Structures, Wiley, New York (1957) (Russian translation published by Izd. Inostr. Lit., Moscow (1960)).
[38]J. C. Slater, Quantum Theory of Atomic Structure, Vols. I and II, McGraw-Hill, New York (1960).
[39]I. P. Grant, Adv. Phys. **19**, 747 (1970).
[40]C. Froese, Can. J. Phys. **41**, 1895 (1963).
[41]D. F. Mayers and F. O'Brien, J. Phys. B **1**, 145 (1968).
[42]C. C. J. Roothaan, Rev. Mod. Phys. **23**, 69 (1951).
[43]C. C. J Roothaan, Rev. Mod. Phys. **32**, 179 (1960).
[44]C. C. J. Roothaan and P. S. Bagus, Methods Comput. Phys. **2**, 47 (1963).
[45]E. Clementi, IBM J. Res. Dev. Suppl. **9**, 2 (1965).
[46]S. Huzinaga, J. Chem. Phys. **42**, 1293 (1965).
[47]W. Eissner, M. Jones, and H. Nussbaumer, Comput. Phys. Commun. **8**, 270 (1974).
[48]I. P. Grant, Comput. Phys. Commun. **17**, 149 (1979).
[49]E. U. Condon and G. H. Shortley, The Theory of Atomic Spectra, Cambridge University Press, London (1935).
[50]M. Blume and R. E. Watson, Proc. R. Soc. London Ser. A **270**, 127 (1962).
[51]W. B. Bambynek *et al.*, Rev. Mod. Phys. **44**, 716 (1972).
[52]B. Swirles, Proc. R. Soc. London Ser. A **152**, 625 (1935).
[53]B. Swirles, Proc. R. Soc. London Ser. A **157**, 680 (1936).
[54]P. A. M. Dirac, Proc. R. Soc. London **117**, 610 (1928).
[55]P. A. M. Dirac, Proc. R. Soc. London **118**, 351 (1928).
[56]C. G. Darwin, Proc. R. Soc. London **118**, 654 (1928).
[57]I. P. Grant, Proc. R. Soc. London **86**, 523 (1965).
[58]Y. K. Kim, Phys. Rev. **154**, 17 (1967).
[59]Y. K. Kim, Phys. Rev. **159**, 190 (1967).
[60]W. Kohn and L. J. Sham, Phys. Rev. **140**, A1133 (1965).
[61]R. D. Cowan *et al.*, Phys. Rev. **144**, 5 (1966).
[62]F. Herman, J. P. Van Dyke, and I. P. Ortenburger, Phys. Rev. Lett. **22**, 807 (1969).
[63]R. Gáspár, Acta Phys. Acad. Sci. Hung. **3** (1954).
[64]J. C. Slater and K. H. Johnson, Phys. Rev. B **5**, 844 (1972).
[65]T. M. Wilson, J. M. Wood, and J. C. Slater, Phys. Rev. A **2**, 620 (1970).
[66]M. S. Gopinathan, M. A. Whitehead, and R. Bogdanović, Phys. Rev. A **14**, 1 (1976).
[67]D. A. Liberman, D. T. Cromer, and J. T. Waber, Phys. Rev. **137**, A27 (1965).
[68]R. D. Cowan and J. B. Mann, in: Atomic Physics 2, Plenum Press, New York (1971), p. 215.
[69]D. T. Cromer and D. A. Liberman, J. Chem. Phys. **53**, 1891 (1970).
[70]C. P. Bhalla, Nucl. Instrum. Methods **90**, 149 (1970).
[71]T. E. H. Walker and J. T. Waber, J. Phys. B **7**, 674 (1974).
[72]R. Latter, Phys. Rev. **99**, 510 (1955).
[73]K.-N. Huang *et al.*, At. Data Nucl. Data Tables **18**, 243 (1976).
[74]D. R. Hartree, Rep. Prog. Phys. **11**, 113 (1948).
[75]A. O. Williams, Phys. Rev. **58**, 723 (1940).
[76]J. P. Desclaux, At. Data Nucl. Data Tables **12**, 311 (1973).
[77]J. A. Bearden and A. F. Burr, Rev. Mod. Phys. **39**, 125 (1967).
[78]D. F. Mayers, Proc. R. Soc. London Ser. A **241**, 93 (1957).
[79]T. C. Tucker *et al.*, Phys. Rev. **174**, 118 (1968).
[80]E. Arndt, E. Hartmann, and G. Zschornack, Phys. Lett. **A83**, 164 (1981).
[81]Tablitsy fizicheskikh velichin. Spravochnik (Tables of Physical Quantitites. Handbook), Atomizdat, Moscow (1976).
[82]F. P. Larkins, "Transition energies," in: Atomic Inner-Shell Processes, Vol. 1, Academic Press, New York (1975), p. 377.
[83]T. Koopmans, Physica **1**, 104 (1933).
[84]A. M. Desiderio and W. R. Johnson, Phys. Rev. A **3**, 1267 (1971).
[85]C. A. Coulson and F. A. Gianturco, J. Phys. B **1**, 605 (1968).
[86]F. P. Larkins, J. Phys. B **4**, 1 (1971).
[87]F. P. Larkins, J. Phys. B **6**, 14 (1973).
[88]F. P. Larkins, J. Phys. B **6**, 2450 (1973).
[89]R. L. Watson, F. E. Jenson, and T. Chiao, Phys. Rev. A **10**, 1230 (1974).
[90]D. A. Liberman, Phys. Rev. **171**, 1 (1968).
[91]L. J. Sham and W. Kohn, Phys. Rev. **145**, 561 (1966).
[92]D. A. Liberman, Phys. Rev. B **2**, 244 (1970).
[93]J. F. McGilp and P. Weighman, J. Phys. B **13**, 1953 (1980).
[94]R. L. Kauffman *et al.*, Phys. Rev. Lett. **31**, 621 (1973).
[95]A. A. Radtsig and B. N Smirnov, Spravochnik po atomnoĭ i molekulyarnoĭ fizike (Handboook of Atomic and Molecular Physics), Atomizdat, Moscow (1980).
[96]D. L. Matthews, B. M. Johnson, and C. F. Moore, At.

Data Nucl. Data Tables **15**, 41 (1975).
[97]C. P. Bhalla, Phys. Rev. A **8**, 2877 (1973).
[98]H. D. Beetz *et al.*, in: Proc. of the Intern. Conf. on Inner Shell Ionization Phenomena and Future Applications, Atlanta, 1973, U. S. Atomic Energy Commission Report N CONF-720404, Oak Ridge, Tenn. (1973), p. 1374.
[99]G. Zschornack, Preprint E7-82-375 [in English], JINR, Dubna (1982).
[100]H.-U. Siebert *et al.*, Opt. Spektrosk. **42**, 1012 (1977).
[101]G. Zschornack *et al.*, Opt. Spektrosk. **47**, 430 (1979).
[102]A. E. Lindh and O. Lundquist, Ark. Mat. Fys. **18**, 3 (1924).
[103]O. I. Sumbaev and A. F. Mezentsev, Zh. Eksp. Teor. Fiz. **50**, 859 (1965) [Sov. Phys. JETP **23**, 568 (1966)].
[104]B. G. Gokhale, R. B. Chesler, and F. Boehm, Phys. Rev. Lett. **18**, 957 (1967).
[105]P. L. Lee, F. Boehm, and P. Vogel, Phys. Rev. A **9**, 614 (1973).
[106]N. A. Dyson, x-Rays in Atomic and Nuclear Physics, Longman, London (1973).
[107]F. Boehm, "Isotope shifts and hyperfine interactions," in: Atomic Inner-Shell Processes, Vol. 1, Academic Press, New York (1975), p. 411.
[108]E. V. Petrovich *et al.*, Zh. Eksp. Teor. Fiz. **55**, 745 (1969). [Sov. Phys. JETP **28**, 385 (1969)].
[109]E. V. Petrovich *et al.*, Zh. Eksp. Teor. Fiz. **61**, 1756 (1971) [Sov. Phys. JETP **34**, 935 (1972)].
[110]P. L. Lee, E. C. Seltzer, and F. Boehm, Phys. Lett. **29** (1972).
[111]M. Siegbahn and W. Stenström, Phys. Z. **17**, 48, 318 (1916).
[112]D Coster, Philos. Mag. **43**, 1070, 1088 (1922).
[113]F. K. Richtmyer and R. D. Richtmyer, Phys. Rev. **34**, 574 (1929).
[114]W. Stenström, Ann. Phys. (Leipzig) **57**, 347 (1918).
[115]E. Hjalmar, Z. Phys. **1**, 439 (1920).
[116]F. R. Hirsh, Jr., Phys. Rev. **38**, 914 (1931).
[117]G. Wentzel, Z. Phys. **6**, 437 (1921).
[118]G. Wentzel, Z. Phys. **31**, 445 (1925).
[119]M. J. Druyvesteyn, Z. Phys. **43**, 707 (1927).
[120]B. B. Ray, Philos. Mag. **8**, 772 (1928).
[121]E. H. Kennard and E. G. Ramberg, Phys. Rev. **46**, 1040 (1934).
[122]D. Coster and R. Del Kronig, Physica **13** (1935).
[123]F. R. Hirsh, Jr., Phys. Rev. **50**, 191 (1936).
[124]Y. Cauchois and C. Senemaud, Wavelengths of x-Ray Emission Lines and Absorption Edges, Pergamon Press, Oxford (1979).
[125]H. F. Beyer, GSI-Report 79-6, Darmstadt (1979).
[126]T. Åberg, Spectra and Electronic Structure of Matter, Vol. 1, Munich (1973), p. 1.
[127]T. Åberg, "Two-photon emission, the radiation Auger effect and the double Auger process," in: Atomic Inner-Shell Processes, Vol. 1, Academic Press, New York (1975), p. 353.
[128]F. Bloch, Phys. Rev. **48**, 187 (1935).
[129]A. Meisel, G. Leonhard, and R. Szargan, Röntgenstrahlen und chemische Bindung, Geest and Portig, Leipzig (1977).
[130]R. L Barinski and W. I. Nefedow, Röntgenspektroskopische Bestimmung der Atomladungen in Molekülen, Geest und Portig, Leipzig (1969).
[131]J. Valasek, Phys. Rev. **52**, 250 (1937); **53**, 274 (1938).
[132]T. Åberg, see Ref. 98, p. 1509.
[133]T. A. Carlson *et al.*, Phys. Rev. **169**, 27 (1968).
[134]T. A. Carlson and C. W. Nestor, Jr., Phys. Rev. A **8**, 2887 (1973).
[135]T. Åberg, Phys. Rev. A **4**, 1735 (1971).
[136]T. A. Carlson, W. E. Moddeman, and M. O. Krause, Phys. Rev. A **5**, 1406 (1970).
[137]M. O. Krause, J. Phys. C **32**, 4–67 (1971).
[138]M. O. Krause, T. A. Carlson, and R. D. Dismukes, Phys. Rev. **170**, 37 (1968).
[139]T. N. Chang, T. Ishihava, and R. T. Poe, Phys. Rev. Lett. **27**, 838 (1971).
[140]M. O. Krause, see Ref. 98, p. 1586.
[141]F. Wuilleumier and M. O. Krause, x-Ray Spectra and Structure of Matter, Vol. 1, Munich (1973), p. 397.
[142]A. N. Nigam and R. B. Mathur, see Ref. 98, p. 1698.
[143]J. Chadwick, Philos. Mag. **24**, 594 (1912).
[144]J. Chadwick, Philos. Mag. **25**, 193 (1913).
[145]A. S. Russel and J. Chadwick, Philos. Mag. **27**, 112 (1914).
[146]J. J. Thomson, Philos. Mag. **28**, 620 (1914).
[147]L. Meitner, Z. Phys. **9**, 131 (1922).
[148]H. Robinson, Proc. R. Soc. London Ser. A **104**, 455 (1923).
[149]P. Auger, J. Phys. Radium **6**, 205 (1925).
[150]P. Auger, Ann. Phys. (Paris) **6**, 183 (1926).
[151]D. Burch, L. Wilets, and W. E. Meyerhof, Phys. Rev. A **9**, 1007 (1974).
[152]P. H. Mokler and F. Folkman, "x-ray production in heavy ion–atom collisions," in: Structure and Collisions of Ions and Atoms, Springer-Verlag, Berlin (1978), p. 201.
[153]J. C. Slater, Phys. Rev. **36**, 57 (1930).
[154]R. L Watson *et al.*, Phys. Rev. A **15**, 914 (1977).
[155]P. Richard, "Ion–atom collisions," in: Atomic Inner-Shell Processes, Vol. 1, Academic Press, New York (1975), p. 74.
[156]P. Richard, in: Scientific and Industrial Applications of Small Accelerators, Publ. No. 76 CH 1175-9 NPS, IEEE, New York (1976), p. 293.
[157]W. Wölfli *et al.*, in: Proc. of the Sec. Intern. Conf. on Inner-Shell Ionization Phenomena, Invited Papers, Freiburg (1976), p. 272.
[158]E. U. Condon and G. H. Shortley, The Theory of Atomic Spectra, Cambridge University Press, London (1957).
[159]B. W. Shore and D. H. Menzel, Principles of Atomic Spectra, Wiley, New York (1968).
[160]M. Mizushima, Quantum Mechanics of Atomic Spectra and Atomic Structure, Benjamin, New York (1970).
[161]I. I. Sobel'man, Vvedenie v teoriyu atomnykh spektrov (Introduction to the Theory of Atomic Spectra), Nauka, Moscow (1977).
[162]F. P. Larkins, J. Phys. B **4**, 129 (1971).
[163]S. A. Moszkowski, "Theory of multipole radiation," in: Alpha-, Beta- and Gamma-Ray Spectroscopy, Vol. II, North-Holland, Amsterdam (1965), p. 863.
[164]J. H. Scofield, Phys. Rev. **179**, 9 (1969).
[165]J. H. Scofield, Phys. Rev. A **9**, 1401 (1974).
[166]M. E. Rose, Multipole Fields, Wiley, New York (1955).
[167]F. A. Babushkin, Acta Phys. Pol. **25**, 749 (1964).
[168]F. A. Babushkin, Opt. Spektrosk. **19**, 3 (1965).
[169]F. A. Babushkin, Opt. Spektrosk. **19**, 879 (1965).
[170]F. A. Babushkin, Acta Phys. Pol. **31**, 459 (1967).
[171]H. P. Kelly, "Many-body perturbation approaches to the calculation of transition probabilities," in: Atomic Inner-Shell Processes, Vol. I, Academic Press, New York (1975), p. 331.
[172]J. C. McGuire, Phys. Rev. **185**, 1 (1969).
[173]J. C. McGuire, Phys. Lett. **A33**, 288 (1970).
[174]J C. McGuire, Phys. Rev. A **2**, 273 (1970).
[175]J. C. McGuire, Phys. Rev. A **3**, 587 (1971).
[176]J. C. McGuire, Phys. Rev. A **5**, 1043 (1972).
[177]J. C. McGuire, Phys. Rev. A **6**, 851 (1972).
[178]D. L. Walters and C. P. Bhalla, At. Data **3**, 301 (1971).
[179]D. L. Walters and C. P. Bhalla, Phys. Rev. A **3**, 1919 (1971).
[180]D. L. Walters and C. P. Bhalla, Phys. Rev. A **4**, 2164 (1971).
[181]C. P. Bhalla, Phys. Rev. A **2**, 2575 (1970).
[182]C. P Bhalla, J. Phys. B **3**, 916 (1970).
[183]C. P. Bhalla, Phys. Rev. A **6**, 1409 (1972).
[184]C. P. Bhalla, Phys. Lett. **A45**, 19 (1973).
[185]C. P. Bhalla and M. Hein, Phys. Rev. Lett. **30**, 39 (1973).

[186]H. R. Rosner and C. P. Bhalla, Z. Phys. **231**, 347 (1970).
[187]C. C. Lu, F. B. Malid, and T. A. Carlson, Nucl. Phys. A175, 289 (1971).
[188]S. T. Manson and D. J. Kennedy, At. Data Nucl. Data Tables **14**, 111 (1974).
[189]R. J. Walen, C. Brianson, and M. Valadares, see Ref. 98, p. 1906.
[190]D. L. Matthews, B. M. Johnson, and C. G Moore, At. Data Nucl. Data Tables **15**, 41 (1975).
[191]T. A. Carlson *et al.*, At. Data **2**, 63 (1970).
[192]C. E. Moore, Atomic Energy Levels, Vol. I; Circular of the NBS-467 (1949).
[193]C. E. Moore, Atomic Energy Levels, Vol. II; Circular of the NBA-467 (1952).
[194]C. E. Moore, Atomic Energy Levels, Vol. III; Circular of the NBS-467 (1958).
[195]C. E. Moore, Ionization Potentials and Ionization Limits Derived from Analyses of Optical Spectra, NSRDS-NBS 34, U. S. Government Printing Office, Washington, D. C. (1970).
[196]A. R. Striganov and N. S. Sventitskiĭ, Tablitsy spektral'nykh liniĭ neĭtral'nykh i ionizovannykh atomov (Tables of Spectral Lines of Neutral and Ionized Atoms), Atomizdat, Moscow (1966).
[197]R. L. Kelly and D. E. Harrison, Jr., At. Data **3**, 177 (1971).
[198]V. P. Ryshkov, Zh. Obshch. Khim. **49**, 2161 (1979).
[199]K. Alder, G. Bauer, and U. Raff, Helv. Phys. Acta **45**, 765 (1972).
[200]G. N. Ogurtsov, Rev. Mod. Phys. **44**, 1 (1972).
[201]M. E. Rudd, see Ref. 98, p. 1485.
[202]G. Wentzel, Z. Phys. **43**, 524 (1927).
[203]N. F. Mott and H. S. W. Massey, The Theory of Atomic Collisions, Oxford University Press, London (1965).
[204]K. N. Huang, J. Phys. B **11**, 787 (1978).
[205]C. Møller, Z. Phys. **70**, 786 (1931).
[206]H. A. Bethe and E. E. Salpeter, Quantum Mechanics of One- and Two-Electron Atoms, Springer-Verlag, Berlin (1957).
[207]H. Körber and W. Mehlhorn, Z. Phys. **191**, 217 (1966).
[208]M. O. Krause *et al.*, Phys. Lett. A31, 81 (1970).
[209]L. O. Werme, T. Bergmark, and K. Siegbahn, Phys. Scr. **6**, 141 (1972).
[210]C. P. Bhalla and D. L. Walters, see Ref. 98, p. 1572.
[211]N. M. Blininov *et al.*, Preprint 9-124-09 [in Russian], JINR, Dubna (1979).
[212]W. Henneberg, Z. Phys. **86**, 592 (1933).
[213]E. Merzbacher and H. W. Lewis, in: Handbuch der Physik, Vol. 34, Springer-Verlag, Berlin (1958), p. 166.
[214]G. S. Khandelwal and E. Merzbacher, Phys. Rev. **151**, 12 (1966).
[215]G. S. Khandelwal, B. H. Choi, and E. Merzbacher, At. Data **1**, 103 (1969).
[216]J. Bang and J. M. Hansteen, K. Dan. Vidensk. Selsk. Mat.-Fys. Medd. **31**, 13 (1959).
[217]M. Gryzinski, Phys. Rev. **138**, A305, A322, A336 (1965).
[218]E. Gerjuoy, Phys. Rev. **148**, 54 (1966).
[219]J. D. Garcia, E. Gerjuoy, and J. Wekler, Phys. Rev. **165**, 66 (1968).
[220]J. D. Garcia, Phys. Rev. A **1**, 280, 1402 (1970).
[221]J. D. Garcia, Phys. Rev. A **4**, 955 (1971).
[222]L. Vriens, Proc. R. Soc. London **90**, 935 (1966).
[223]H.-U. Siebert *et al.*, Preprint R9-10197 [in Russian], JINR Dubna (1976).
[224]Y. Hahn, Phys. Rev. A **13**, 1326 (1976).
[225]C. J. Powell, Rev. Mod. Phys. **48**, 33 (1976).
[226]M. R. H. Rudge and S. B. Schwartz, Proc. Phys. Soc. London **88**, 563, 579 (1966).
[227]W. J. Lotz, Opt. Soc. Am. **57**, 873 (1967).
[228]W. J. Lotz, Z. Phys. **216**, 341 (1968).
[229]E. Stingl, J. Phys. B **5**, 1160 (1972).
[230]D. L. Moores, J. Phys. B **11**, 403 (1978).
[231]L. B. Golden and D. H. Sampson, J. Phys. B **10**, 2229 (1977).
[232]G. Peach, J. Phys. B **4**, 1670 (1971).
[233]J. B. Hasted, Physics of Atomic Collisions, Butterworths, London (1964) (Russian translation published by Mir, Moscow (1965), p. 337).
[234]K. L. Aitken and M. F. A. Harrison, J. Phys. B **4**, 1176 (1971).
[235]S. O. Martin, B. Peart, and K. T. Dolder, J. Phys. B **1**, 577 (1968).
[236]D. H. Crandall *et al.*, ORNL/TM-7020 (1979).
[237]D. H. Crandall, Phys. Scr. **23**, 153 (1981).
[238]E. D. Donets and V. P. Ovsyannikov, Preprint R7-10780 [in Russian], JINR, Dubna (1977).
[239]E. D. Donets and V. P. Ovsyannikov, Preprint R7-80-404 [in Russian], JINR, Dubna (1980).
[240]E. D. Donets and V. P. Ovsyannikov, Preprint R7-9799 [in Russian], JINR, Dubna (1976).
[241]E. D. Donets and A. I. Pikin, Zh. Eksp. Teor. Fiz. **70**, 2025 (1976) [Sov. Phys. JETP **43**, 1057 (1976)].
[242]E. D. Donets and A. I. Pikin, Zh. Tekh. Fiz. **42**, 2373 (1975) [Sov. Phys. Tech. Phys. **20**, 1477 (1976)].
[243]J. J. Thomson, Philos. Mag. **23**, 449 (1912).
[244]W. Lotz, Z. Phys. **220**, 466 (1969).
[245]V. A. Bazylev and M. I. Chibisov, Preprint IAÉ-3125 (1979).
[246]V. A. Bazylev and M. I. Chibisov, Preprint IAÉ-3152 (1978).
[247]D. H. Sampson and L. B. Golden, J. Phys. B **11**, 541 (1978).
[248]L. B. Golden, D. H. Sampson, and K. Omidvar, J. Phys. B **11**, 3235 (1978).
[249]D. L. Moores, L. B. Golden, and D. H. Sampson, J. Phys. B **13**, 385 (1980).
[250]A. Burgess, in: Proc. of the Third Intern. Conf. on the Physics of Electron and Atomic Collisions, North-Holland, London (1963), p. 237.
[251]A. Burgess, in: Proc. of the Symposium on Atomic Collision Processes in Plasmas, Culham; A. E. R. E. Report No. 4818 (1964).
[252]A. Burgess *et al.*, Mon. Not. R. Astron. Soc. **179**, 275 (1977).
[253]Y. Hahn and K. M. Watson, Phys. Rev. A **7**, 491 (1974).
[254]P. P. Szydlik and A. E. S. Green, Phys. Rev. A **9**, 1885 (1974).
[255]A. E. S. Green, D. L. Sellin, and A. S. Zachor, Phys. Rev. **184**, 1 (1969).
[256]H. Bethe, Ann. Phys. (Leipzig) **5**, 325 (1930).
[257]T. A. Carlson, W. E. Hunt, and M. O. Krause, Phys. Rev. **151**, 41 (1966).
[258]K. Omidvar and A. H. Khateeb, J. Phys. B **6**, 1507 (1972).

Translated by Julian B. Barbour